# METRICS ON MARKOV EQUIVALENCE CLASSES FOR EVALUATING CAUSAL DISCOVERY ALGORITHMS

#### Jonas Wahl

Technische Universität Berlin
Berlin, Germany
and
Deutsches Zentrum für Luft- und Raumfahrt (DLR)
Institut für Datenwissenschaften
Jena, Germany.
wahl@tu-berlin.de

## Jakob Runge

Deutsches Zentrum für Luft- und Raumfahrt (DLR)
Institut für Datenwissenschaften
Jena, Germany.
and
Technische Universität Berlin
Berlin, Germany.
jakob.runge@dlr.de

# **ABSTRACT**

Many state-of-the-art causal discovery methods aim to generate an output graph that encodes the graphical separation and connection statements of the causal graph that underlies the data-generating process. In this work, we argue that an evaluation of a causal discovery method against synthetic data should include an analysis of how well this explicit goal is achieved by measuring how closely the separations/connections of the method's output align with those of the ground truth. We show that established evaluation measures do not accurately capture the difference in separations/connections of two causal graphs, and we introduce three new measures of distance called s/c-distance, Markov distance and Faithfulness distance that address this shortcoming. We complement our theoretical analysis with toy examples, empirical experiments and pseudocode.

# 1 Introduction

Inferring causal relations from observational data in the form of a *causal graph* is a highly challenging task for which causality researchers have proposed numerous automatized methods in the past three decades. While the assumptions on which these methods rely, differ widely, many of the existing approaches, including the PC-algorithm [Spirtes et al., 1993], stablePC [Colombo and Maathuis, 2014], consistentPC [Li et al., 2019], PCMCI+ [Runge, 2020], LPMCI [Gerhardus and Runge, 2020], FCI [Spirtes et al., 2013], and GES [Chickering, 2003] share two important commonalities.

Firstly, if their assumptions are fulfilled, these methods are provably able to infer the correct causal graph up to *Markov equivalence* in the infinite sample limit. More precisely, these approaches assume that the process that generating the data to which they are being applied, can be represented by a causal graph that belongs to a predefined class of graphs  $\mathbb{G}$ . For instance, this class of graphs is  $\mathbb{G} = \{\text{directed acyclic graphs (DAGs)}\}\$  for the PC-algorithm and GES,  $\mathbb{G} = \{\text{maximal ancestral graphs (MAGs)}\}\$  for FCI and  $\mathbb{G} = \{\text{time series DAGs (tsDAGs)}\}\$  for PCMCI+. The class of graphs  $\mathbb{G}$  is equipped with a notion of *separation*, that is, a graphical criterion that specifies whether two nodes X, Y in a graph are *separated* or *connected* by a subset of nodes  $\mathcal{S}$ . The most commonly used type of separation is d-separation for DAGs (or tsDAGs) [Spirtes et al., 1993] which generalizes to m-separation for MAGs [Zhang, 2008], but other types of separation also exist, e.g.  $\sigma$ -separation for cyclic graphs, see [Bongers et al., 2021]. Two graphs within the class  $\mathbb{G}$  are then called *Markov equivalent* if they imply exactly the same separation/connection statements, and all of the methods above aim to infer the Markov equivalence class of the 'ground truth' graph that underlies the data-generating process.<sup>1</sup>

The second commonality shared by the algorithms mentioned above, is that all of them have been introduced alongside a range of empirical simulations that compare their output graphs to known ground truths. The difference between

<sup>&</sup>lt;sup>1</sup>Methods that make inferences beyond the Markov equivalence class also exist (e.g., LiNGaM [Shimizu et al., 2006]), but require additional parametric modelling assumptions.

the output and the ground truth is usually measured by means of the structural Hamming distance (SHD) [Acid and Campos, 2003, Tsamardinos et al., 2006], the structural intervention distance (SID) [Peters and Bühlmann, 2015], false positive and false negative rates for edge detection, or measures of predictive performance, see e.g [Liu et al., 2010, Biza et al., 2020].

The purpose of this work is to argue the following point: given that the goal of many methods is to infer the Markov equivalence class of the ground truth graph, a performance evaluation should include an analysis of how close the method is to achieving *this exact goal*. Hence, it should include a comparison of the output graph's implied separation/connection statements to those of the ground truth graph. Current evaluation metrics, even though all of them have merits of their own, do not provide such a comparison. For instance, graphs that are similar in SHD or SID can imply very different separations, see Section 3.3.

**Contributions** To address this shortcoming, we introduce three new distance measures called s/c-distance. Markov distance (or c-distance) and Faithfulness distance (or s-distance).<sup>2</sup> We prove that the s/c-distance is a metric on the set of Markov equivalence classes of causal graphs in the strict mathematical sense, and point out that Markov and Faithfulness distance are the analogues of false negative and false positive rates for separation and connection statements. In a simulated experiment in which the data-generation process is built such that the joint distribution  $P_{\mathbf{X}}$  is Markovian and faithful on a ground truth graph  $\mathcal{G}_0$ , the Markov distance measures how far  $P_{\mathbf{X}}$  is from being Markovian on a method's output graph G. Similarly, the Faithfulness distance measures how far the pair  $P_X$  is from being faithful on  $\mathcal{G}$ . A practical challenge for the introduced measures is that their computation requires the evaluation of *all* conditional (in)dependence statements which is computationally infeasible except for reasonably small graphs. We therefore propose an approximation scheme that only computes separations/connections for separating sets of low order and randomly draws a limited number of separation/connection statements for each higher order term. In empirical experiments, we find that this yields a very close approximation, see Section 3. We also describe how the s/c-distance can be leveraged for robustness checks, even when no ground truth data is available, by estimating how strongly changes in a method's hyperparameters affect the separations/connections of their output. As an additional baseline for statistical tests of conditional independence in the context of causal graphical models, we also discuss connection false negative and separation false positive rates that quantify how well a test is able to see the separations/connections of the ground truth. Our theoretical arguments will be complemented by toy examples and empirical experiments in which we compare existing evaluation methods to our proposed ones as well as a Python implementation of our metrics.

**Strengths and Limitations** We argue in this work that our proposed notions of distance capture the actual target of many causal discovery methods, the Markov equivalence class, more accurately than existing metrics. Moreover, s/c-, Markov and Faithfulness distance are well-defined for any class of graphs that is equipped with an appropriate notion of separation, and, due to its symmetry, the s/c-distance can also be used to compare outputs of a method at different hyperparameter values or graphs that were returned by two different approaches. However, the fact that the introduced distances only take into account the Markov equivalence classes of the graphs under investigation, means by definition that they are not able to distinguish members of the same equivalence class. For comparisons within a Markov equivalence class, one needs to resort to other metrics to quantify differences between class members.

Related Work We already mentioned the articles [Acid and Campos, 2003, Tsamardinos et al., 2006], [Peters and Bühlmann, 2015] and [Liu et al., 2010, Biza et al., 2020] that introduced the SHD, SID and predictive performance metrics. The SID was recently generalized to a broader class of *adjustment identification distances* in [Henckel et al., 2024]. In addition, several recent works address method evaluation and causal graph falsification. Faller et al. [2023] propose a criterion for evaluating causal discovery algorithms in the absence of a ground truth which quantifies the compatibility of causal graphs over different subsets of variables. Pitchforth and Mengersen [2013] review methods to validate expert-elicited Bayesian networks, Machlanski et al. [2023] discuss causal model evaluation in the context of causal effect estimation, and Eulig et al. [2023] develop a permutation-based test for causal graph falsification. Reisach et al. [2021, 2023] provide a baseline comparison for causal discovery methods based on variance sorting as well as a critique of current methods to generate simulated data, while Parikh et al. [2022] introduce a method that generates synthetic data from the empirical distribution of a real-world dataset. A function to compute all separation statements from a causal graph is implemented in the R-package *Dagitty* [Textor et al., 2016], the Python package *networkx* and the Python package *Tigramite* [Runge et al., 2019].

<sup>&</sup>lt;sup>2</sup>s and c are short for separation and connection.

# 2 Notations and Preliminaries

In this work,  $\mathbf{X}$  denotes a set of random variables,  $\mathcal{D}_n = \{\mathbf{x}_1, \dots, \mathbf{x}_n\}$  is a collection of n samples of  $\mathbf{X}$ , and  $\mathcal{M}$  is our generic symbol for a causal discovery method, e.g.  $\mathcal{M}$  could be a stand-in for the PC-algorithm.  $\mathbb{G}$  will be our generic symbol for a class of causal graphs understood to have the same set of nodes. In the later parts of this work, T will be a generic conditional independence test ( for instance the partial correlation test), and  $\alpha$  is the test's significance level. We will often pair these together as  $(T,\alpha)$ . Different types of causal graphs come with their own notion of graphical separation, that is to say, a criterion that decides for any graph in the class  $\mathbb{G}$ , whether a triple  $(X,Y,\mathcal{S})$  with  $X,Y \in \mathbf{X}$ ,  $X \neq Y$  and  $\mathcal{S} \subset \mathbf{X} \setminus \{X,Y\}$  is separated or connected. The most common notions of separation are d-separation for DAGs, m-separation for MAGs, or  $\sigma$ -separation for cyclic graphs [Bongers et al., 2021]. Most statements in this work don't depend on the type of graph as long as consistently uses the corresponding notion of separation (respectively connection). We will use the following sets throughout this work:

- $\mathcal{C}$  is the set of triples  $(X,Y,\mathcal{S})$  with  $X,Y\in\mathbf{X},\ X\neq Y$  and  $\mathcal{S}\subset\mathbf{X}\setminus\{X,Y\}$ . We implicitly identify triples  $(X,Y,\mathcal{S})\sim(Y,X,\mathcal{S})$ .
- $\mathcal{C}^k$  is the set of triples  $(X,Y,\mathcal{S})\in\mathcal{C}$  with  $|\mathcal{S}|=k$ . In particular, if  $\mathbf{X}$  consists of N variables, then  $\mathcal{C}=\bigsqcup_{k=0}^{N-2}\mathcal{C}^k$ .
- If  $\mathcal{G}_0$  is a graph with an appropriate notion of separation, we write  $\mathcal{C}_{con}(\mathcal{G}_0) = \{(X,Y,\mathcal{S}) \in \mathcal{C} \mid X \bowtie_{\mathcal{G}_0} Y | \mathcal{S} \}$  for the set of connection statements in  $\mathcal{G}_0$  and  $\mathcal{C}_{sep}(\mathcal{G}_0) = \{(X,Y,\mathcal{S}) \in \mathcal{C} \mid X \bowtie_{\mathcal{G}_0} Y | \mathcal{S} \}$  for the set of its separation statements. We also write  $\mathcal{C}^k_{con}(\mathcal{G}_0)$  respectively  $\mathcal{C}^k_{sep}(\mathcal{G}_0)$ , for the set of connection (separation) statements of order k, i.e. with  $|\mathcal{S}| = k$ .

We will call two causal graphs  $\mathcal{G}, \mathcal{H} \in \mathbb{G}$  *Markov equivalent* if they share the same separations, i.e.  $\mathcal{C}_{sep}(\mathcal{G}) = \mathcal{C}_{sep}(\mathcal{H})$  (or equivalently if  $\mathcal{C}_{con}(\mathcal{G}) = \mathcal{C}_{con}(\mathcal{H})$ ). If  $\mathcal{G}$  is causal graph with an appropriate notion of separation, we define the separation indicator function  $\iota_{\mathcal{G}}: \mathcal{C} \to \{0,1\}$  by

$$\iota_{\mathcal{G}}(X, Y, \mathcal{S}) = \begin{cases} 1 & \text{if } X \bowtie_{\mathcal{G}} Y | \mathcal{S} \\ 0 & \text{else.} \end{cases}$$

# 3 Evaluation Metrics in the Presence of a Ground Truth

Whenever a new causal structure learning method is introduced, the run-of-the-mill procedure for empirical performance analysis is to compare the method's output graph to a known ground truth graph which underlies the data-generation process. Standard measures of comparison include

- the *structural Hamming distance (SHD)* [Acid and Campos, 2003, Tsamardinos et al., 2006], which penalizes the output graph for every wrongly added or wrongly deleted edge and wrong edge orientations, see Appendix 3.3 for a reminder of its formal definition;
- the *structural intervention distance (SID)* [Peters and Bühlmann, 2015], which, roughly speaking, counts the number of node pairs for which the output graph  $\mathcal{G}$  returns adjustment sets for estimating interventional distributions that are invalid in the ground truth graph  $\mathcal{G}_0$ , see Appendix 3.3 for details;
- measures of predictive performance, see e.g. [Liu et al., 2010, Biza et al., 2020], even though these have seemingly not been adapted on a broad scale so far.

All these measures have their own strengths and limitations. The SHD is easy to compute, but captures only local differences between two graphs and does not have any straightforward causal meaning. The SID is inherently causal and has a purely graphical characterization [Peters and Bühlmann, 2015, Proposition 6] that is very useful for practical computations. On the other hand, it is only directly defined for DAGs, whereas most algorithms output graphical representations of Markov equivalence classes, e.g. CPDAGs. To compute the SID for CPDAGs, one therefore has to resort to worst and best case estimates across equivalence class members [Peters and Bühlmann, 2015, Section 2.4]. The SID is also asymmetric (i.e. in general  $SID(\mathcal{G},\mathcal{H}) \neq SID(\mathcal{H},\mathcal{G})$ ). We will compare SHD and SID to our proposed measures of distance below in Subsection 3.3, and see that two graphs can be close in both SHD and SID whilst their separations differ significantly. Predictive performance measures such as STARS [Liu et al., 2010] are useful for cross-validation and model selection but can, by definition, only capture predictive and not causal claims.

#### 3.1 s/c-Distance

Most causal discovery methods aim to infer the correct Markov equivalence class, or equivalently, the exact separation/connection statements of the causal graph underlying the data-generating process, and provably achieve this task if the method's assumptions are fulfilled and the number of samples is large enough. We argue that empirical performance analyses on finite samples should therefore investigate the correctness of the inferred equivalence class. To that end, we introduce the following measures of distance between causal graphs.

**Definition 3.1.** Consider two causal graphs  $\mathcal{G}_0$ ,  $\mathcal{G}$  over a set  $\mathbf{X}$  of N nodes, equipped with an appropriate notion of separation and define

$$d_{s/c}^k(\mathcal{G}_0,\mathcal{G}) := \frac{1}{|\mathcal{C}^k|} \sum_{(X,Y,\mathcal{S}) \in \mathcal{C}^k} |\iota_{\mathcal{G}_0}(X,Y,\mathcal{S}) - \iota_{\mathcal{G}}(X,Y,\mathcal{S})|$$

for k = 0, ..., N - 2. The s/c-distance up to order K is defined as

$$d_{s/c}^{\leq K}(\mathcal{G}_0, \mathcal{G}) = \frac{1}{K+1} \sum_{k=0}^K d_{s/c}^k(\mathcal{G}_0, \mathcal{G}).$$

If K = N - 2, we simply speak of the **s/c-distance** and write  $d_{s/c}$  instead of  $d_{s/c}^{N-2}$ .

In words, the s/c-distance measures how strongly the separation/connection statements in the set  $\mathcal{B}$  disagree in the two graphs. The following result shows that the s/c-distance is an appealing notion of distance from a theoretical point of view. See Appendix B for its proof.

**Lemma 3.2.** Consider a class of graphs  $\mathbb{G}$  over  $\mathbf{X}$  with an appropriate notion of separation.

Then,  $d_{s/c}(\mathcal{G}_0,\mathcal{G})=0$  if and only if  $\mathcal{G}_0$  and  $\mathcal{G}$  are Markov equivalent. Moreover,  $d_{s/c}$  defines a metric (in the mathematical sense of the word) on the set of Markov equivalence classes over  $\mathbb{G}$ .

- Remark 3.3. Since  $d_{s/c}^k(\mathcal{G}_0,\mathcal{G})$  is bounded by 1,  $d_{s/c}^{\leq K}(\mathcal{G}_0,\mathcal{G})$  is also bounded by 1 (due to the normalization constant  $\frac{1}{K+1}$ ). This value is taken if  $\mathcal{G}_0$  is the fully disconnected and  $\mathcal{G}$  is a fully connected graph.
  - In Lemma 3.2, we can also replace Markov equivalence with the weaker notion of K-th order Markov equivalence: we simply call two graphs  $\mathcal{G}_0$ ,  $\mathcal{G}$  K-th order Markov equivalent if their separations/connections coincide up to order K, that is if  $d_{s/c}^{\leq K}(\mathcal{G}_0,\mathcal{G})=0$ , see [Kocaoglu, 2023]. Then  $d_{s/c}^{\leq K}(\mathcal{G}_0,\mathcal{G})$  is a metric on the set of K-th order Markov equivalence classes, see Appendix B for a proof of this.
  - If one prefers to assign more importance to differences in low order statements than to differences in higher order statements, this can be reflected by introducing a weight  $w_k$ ,  $k=0,\ldots N-2$  and replace the s/c-distance with a weighted version

$$d_{s/c}^{w}(\mathcal{G}_{0},\mathcal{G}) = \frac{1}{\sum_{k} w_{k}} \sum_{k=0}^{K} w_{k} \cdot d_{s/c}^{k}(\mathcal{G}_{0},\mathcal{G}).$$

**Practical Approximation** While theoretically appealing, the full s/c-distance is hard to compute for large graphs, as for N nodes, the total number of triples that would have to be checked is  $|\mathcal{C}| = \frac{N(N-1)}{2} \cdot 2^{N-2}$ . In practice, one therefore needs to restrict oneself to a manageable number of separation/connection statements. We suggest to approximate  $d_{s/c}$  as follows:

- (1) first  $d_{s/c}^{\leq K}$  for a small value of K. That is the compute all terms of orders  $0, \ldots, K$ ;
- (2) To compute higher order terms, we suggest to draw a set  $\mathcal{L}_k$  consisting of  $L_k$  statements uniformly at random from  $\mathcal{C}_k$  for each k > K and to approximate the higher order terms by<sup>3</sup>

$$d_{s/c}^{k}(\mathcal{G}_{0},\mathcal{G})$$

$$\approx \frac{1}{L_{k}} \sum_{(X,Y,\mathcal{S})\in\mathcal{L}^{k}} |\iota_{\mathcal{G}_{0}}(X,Y,\mathcal{S}) - \iota_{\mathcal{G}}(X,Y,\mathcal{S})|.$$

<sup>&</sup>lt;sup>3</sup>Another viable choice would be to also compute *all* statements of order  $k \ge N - K - 2$  since the number of these is again manageable.

Empirical Quality of Approximation As an empirical test, we have drawn two random graphs on N=8 nodes 100 times and compared the full s/c-distance to an approximation with 100 and one with 500 randomly selected triples for higher order terms ( $k \geq 2$ ) (henceforth approximation A and B). Across all experiments, the full s/c-distance and approximation A differed on average by av-diff $_A=6.7\cdot 10^{-3}$  and at most by max-diff $_A=2.7\cdot 10^{-2}$ . The full s/c-distance and approximation B differed on average by av-diff $_B=7.3\cdot 10^{-4}$  and at most by max-diff $_B=3.9\cdot 10^{-3}$ , see also Figure 1 in Appendix F. Analogous experiments with N=12 nodes yielded similar results (av-diff $_A=9\cdot 10^{-3}$ , max-diff $_A=2.8\cdot 10^{-2}$ , av-diff $_B=3.4\cdot 10^{-3}$ , max-diff $_B=1.2\cdot 10^{-2}$ ).

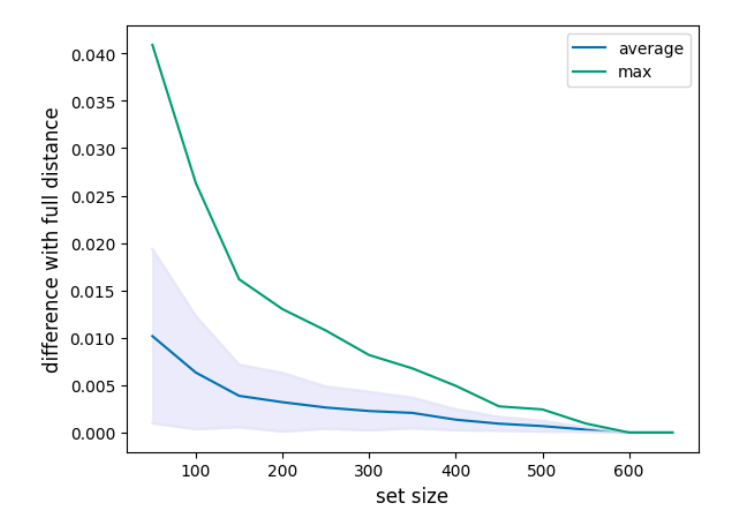


Figure 1: Closeness of the approximation with randomly chosen sets of triples to the full s/c-distance for DAGs on N=8 variables. The blue line shows the average difference (in absolute value) and the green line the maximal difference between the full s/c-distance and its approximation across 100 randomly drawn graphs. The x-axis denotes the number of randomly selected triples per order  $k \ge 2$ .

## 3.2 Markov and Faithfulness Distance

The s/c-distance introduced in the previous subsection is a symmetric notion of distance for two causal graphs to which differences in connections and differences in separations between the two graphs contribute equally. We can also consider separations and connections separately at the price of losing symmetry: we have to specify to which graph the separations or connections that we would like to compare, are referring. This asymmetry is nothing new, as the SID is similarly asymmetric.

**Definition 3.4.** Consider two causal graphs  $\mathcal{G}_0$ ,  $\mathcal{G}$  over the same set of nodes  $\mathbf{X}$ , equipped with an appropriate notion of separation. We first define

$$d_c^k(\mathcal{G}_0,\mathcal{G}) := \frac{1}{|\mathcal{C}_{con}^k(\mathcal{G}_0)|} \sum_{(X,Y,\mathcal{S}) \in \mathcal{C}_{con}^k(\mathcal{G}_0)} \iota_{\mathcal{G}}(X,Y,\mathcal{S}).$$

for  $k = 0, \dots, N - 2$ . Then we call

$$d_c^{\leq K} = \frac{1}{K+1} \sum_{k=0}^{K} d_c^k(\mathcal{G}_0, \mathcal{G}).$$

the **c-distance** or **Markov distance** of  $\mathcal{G}$  to  $\mathcal{G}_0$  of order **K**. If K = N - 2, we just speak of the **c-distance** or **Markov distance** and write  $d_c$  instead of  $d_c^{N-2}$ .

We recall that a distribution  $P_{\mathbf{X}}$  over the node variables  $\mathbf{X}$  is called *Markovian* on a causal graph  $\mathcal{G}$ , if the separation  $X \bowtie_{\mathcal{G}} Y | \mathcal{S}$  on the implies the conditional independence  $X \perp\!\!\!\perp_{P_{\mathbf{X}}} Y | \mathcal{S}$ , and *faithful* on  $\mathcal{G}$  if the converse implication holds as well.

The name 'Markov distance' is justified by the following result. See Appendix B for its proof.

**Lemma 3.5.** Consider two causal graphs  $\mathcal{G}_0$ ,  $\mathcal{G}$  over the same set of nodes  $\mathbf{X}$ , equipped with an appropriate notion of separation. Suppose that  $P_{\mathbf{X}}$  is a distribution on  $\mathbf{X}$  that is Markovian and faithful on the graph  $\mathcal{G}_0$ . Then  $d_c(\mathcal{G}_0,\mathcal{G}) \neq 0$ , if and only if  $P_{\mathbf{X}}$  is not Markovian on  $\mathcal{G}$ .

Consider a simulated experiment to evaluate a causal discovery method  $\mathcal{M}$  which outputs the graph  $\mathcal{G}$ . If the parameters of the data-generation process are chosen in such a way that the Markov property and causal Faithfulness w.r.t to the ground truth graph  $\mathcal{G}_0$  is guaranteed, according to the previous lemma,  $d_c(\mathcal{G}_0,\mathcal{G}) \neq 0$  means that  $P_{\mathbf{X}}$  does not have the Markov property on the output graph. In other words,  $d_c(\mathcal{G}_0,\mathcal{G})$  measures how far the pair  $(\mathcal{G},P_{\mathbf{X}})$  is from being Markovian. As the Markov property is the most fundamental link between the distribution and the graph, a large Markov distance should be a clear warning sign that the algorithm is not performing well (or that the data-generation process is far from being faithful on the ground truth graph).

We can define an analogous notion for separations instead of connections.

**Definition 3.6.** Consider two causal graphs  $\mathcal{G}_0$ ,  $\mathcal{G}$  over the same set of nodes  $\mathbf{X}$ , equipped with an appropriate notion of separation. We first define

$$d_s^k(\mathcal{G}_0,\mathcal{G}) := \frac{1}{|\mathcal{C}_{sep}^k(\mathcal{G}_0)|} \sum_{(X,Y,\mathcal{S}) \in \mathcal{C}_{sep}^k(\mathcal{G}_0)} 1 - \iota_{\mathcal{G}}(X,Y,\mathcal{S}).$$

for  $k = 0, \dots, N - 2$ . Then we call

$$d_s^{\leq K} = \frac{1}{K+1} \sum_{k=0}^K d_s^k(\mathcal{G}_0, \mathcal{G}).$$

the s-distance or Faithfulness distance of  $\mathcal{G}$  to  $\mathcal{G}_0$  of order K. If K=N-2, we just speak of the c- or Faithfulness distance and write  $d_c$  instead of  $d_c^{N-2}$ .

The following result is the analogue of Lemma 3.5 for the Faithfulness distance. See Appendix B for its proof.

**Lemma 3.7.** Consider two causal graphs  $\mathcal{G}_0$ ,  $\mathcal{G}$  over the same set of nodes  $\mathbf{X}$ , equipped with an appropriate notion of separation. Suppose that  $P_{\mathbf{X}}$  is a distribution on  $\mathbf{X}$  that is Markovian and faithful on the graph  $\mathcal{G}_0$ . Then  $d_s(\mathcal{G}_0, \mathcal{G}) \neq 0$  if and only if  $P_{\mathbf{X}}$  is not faithful on  $\mathcal{G}$ .

The name 'Faithfulness distance' is thus motivated by the fact that if  $\mathcal{G}_0$  is a ground truth graph in a simulated experiment, the Faithfulness distance measures the amount of Faithfulness violations in a method's output graph.

Remark 3.8. • Like the s/c-distance before, both the Markov and the Faithfulness distance only depend on the Markov equivalence classes of the two graphs in play.

- At first glance, it might seem like  $d_s(\mathcal{G}_0,\mathcal{G})=d_c(\mathcal{G},\mathcal{G}_0)$  but this is not the case. The crucial difference lies in the normalization constants of the k-th order contributions which need not coincide in  $d_s(\mathcal{G}_0,\mathcal{G})$  and  $d_c(\mathcal{G},\mathcal{G}_0)$ .
- The statements on approximations after Lemma 3.2 can be made analogously for  $d_c$  and  $d_s$ .

Analogy to False Positive and False Negative Rate The term  $d_c^k$  in the Markov distance measures the number of connections of the ground truth graph  $\mathcal{G}_0$  with  $|\mathcal{S}|=k$  that the graph  $\mathcal{G}$  misses ("false negatives") relative to the total number of connections of  $\mathcal{G}_0$  ("positives") with  $|\mathcal{S}|=k$ . Thus, since we scale the Markov distance by  $\frac{1}{N-1}$  we compute the average false negative rate across all orders for separation/connection statements. Similarly, the Faithfulness distance measures the number of separations of the ground truth graph  $\mathcal{G}_0$  with  $|\mathcal{S}|=k$  that the graph  $\mathcal{G}$  mistakes for connections ("false positives"), relative to the total number of separations of  $\mathcal{G}_0$  ("negatives") with  $|\mathcal{S}|=k$ . The Faithfulness distance, can thus be interpreted as the average false positive rate across all orders for separation/connection statements.

## 3.3 A Toy Example to Compare SHD and SID to s/c-Distances

In this subsection, we will compare the different existing graphical comparison measures in the example of the two DAGs  $\mathcal{G}$  and  $\mathcal{H}$  depicted in Figure 2.

To make all involved metrics comparable, we scale SHD and SID by the total number of node pairs, so that the values of all metrics range in the unit interval. We first observe that  $\mathcal G$  and  $\mathcal H$  are very close in SHD as only the edge between  $X_M$  and  $X_{M+1}$  differs in both graphs. Thus, the normalized SHD-value is  $\widetilde{\mathrm{SHD}}(\mathcal G,\mathcal H)=\frac{1}{M(2M-1)}$ . The only node pairs that contribute to  $\mathrm{SID}(\mathcal G,\mathcal H)$  are (M+1,M) and (M,k) with  $k\in\{M+1,\ldots,2M\}$  which are M+1 pairs in total. The normalized SID is thus  $\widetilde{\mathrm{SID}}(\mathcal G,\mathcal H)=\frac{M+1}{2M(2M-1)}$ . The low-order d-separations/connections differ fundamentally between the two graphs. In  $\mathcal G$  any two nodes  $X_i,X_j$  are d-connected, while in  $\mathcal H$  any two nodes  $X_i,X_j$  with i< M

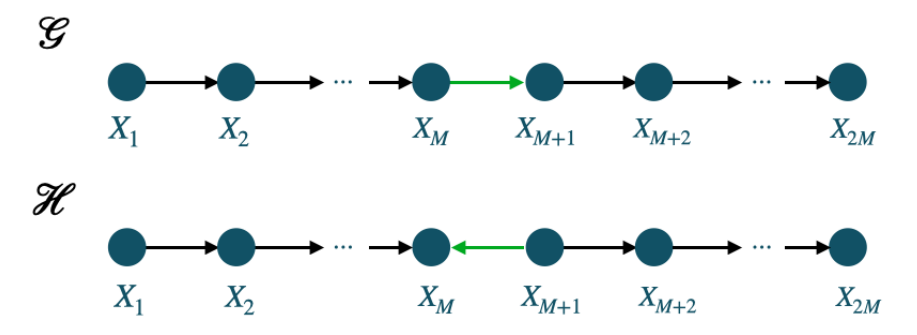


Figure 2: The two example DAGs  $\mathcal{G}$  and  $\mathcal{H}$ . The only difference between the two graphs is the inverted edge orientation between the nodes  $X_M$  and  $X_{M+1}$ .

and j>M are d-separated. These are M(M-1) of the M(2M-1) possible d-separation statements of order zero (i.e. with empty separating set), so that  $d^0_{s/c}(\mathcal{G},\mathcal{H})=\frac{M-1}{2M-1}$ . High-order d-separations/connections on the other hand differ less and less between both graphs. For instance if k=N-2, the all statements  $(X_i,X_j,\mathbf{X}\setminus\{X_i,X_j\})$  agree on both graphs, except for the statement  $(X_{M-1},X_M,\mathbf{X}\setminus\{X_i,X_j\})$  which is a separation on  $\mathcal{G}$  and a connection on  $\mathcal{H}$ . We plot the values of normalized SHD, SID, s/c-distance and Markov distance for  $M=2,\ldots,10$  below in Figure 3. For a plot of  $d^k_{s/c}$ ,  $d^k_c$  and  $d^k_s$  for different values of k in the case M=8 see Figure 13 in the Supplement.

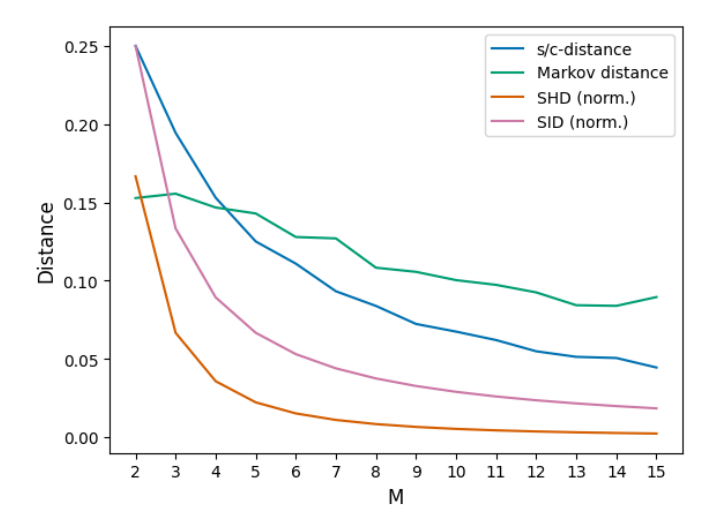


Figure 3: Values of  $d_{s/c}(\mathcal{G},\mathcal{H}), d_c(\mathcal{G},\mathcal{H})$ , normalized SHD and normalized SID in the example of Figure 2 for different values of M (for 2M nodes). To compute  $d_{s/c}$  and  $d_c$ , we have drawn 500 triples randomly for higher order terms. Normalized SHD and SID converge to 0 much faster than s/c-distance and Markov distance with increasing M.

## 3.4 The Challenge of Invalid Output Graphs

Usage of the s/c-distance to compare two graphs  $\mathcal{G}_0$  and  $\mathcal{G}$  requires that both of these graphs are able to decide whether  $(X,Y,\mathcal{S})$  is a separation or a connection statement in the respective graph. For instance, if the applied notion of separation is d-separation, then  $\mathcal{G}_0$  and  $\mathcal{G}$  should be DAGs or CPDAGs. While score-based causal discovery methods like GES [Chickering, 2003], NOTEARS [Zheng et al., 2018], GLOBE [Mian et al., 2021], BCCD [Claassen and Heskes, 2012], parametric methods like LinGaM [Shimizu et al., 2006] or logic-based methods like [Hyttinen et al., 2014] guarantee that their output is either a proper causal graph or a Markov equivalence class, this is no longer true for PC-like algorithms. Due to assumption violations or contradictory independence test results during their execution, these might run into logical conflicts between different orientation rules or they might label unshielded node triples  $X - Y - Z^4$  in the graph as ambiguous. For instance, the conservative PC algorithm of [Ramsey et al., 2006] labels an

<sup>&</sup>lt;sup>4</sup>Recall that a triple (X,Y,Z) of nodes is called unshielded if there are edges between X and Y and between Y and Z, but there is none between X and Z.

unshielded triples X-Y-Z as ambiguous if the middle node Y is in some but not all separating sets that the method found for X and Z. The majority decision rule [Colombo and Maathuis, 2014] labels a triple ambiguous if Y belongs to exactly half of all separating sets found for X and Z. If conflicts or ambiguities occur, the output graph is *invalid* in the sense that it does no longer imply separation/connection statements for arbitrary triples  $(X,Y,\mathcal{S})$ . Hence none of the distance measures introduced in this work can be straightforwardly computed and the SID faces the same problem.

**Dealing with Conflicting Orientations** Since conflicts between different orientation rules are serious errors that flag assumption violations of some form, the most conservative way to treat them in a performance evaluation of a PC-like method is to record the proportion of their occurrence and then disregard graphs with conflicts for further steps. A well-performing method should lead to (a) a low proportion of graphs with conflicts and (b) good results w.r.t. the chosen evaluation metric on its valid output graphs.

**Dealing with Ambiguities** In contrast to conflicting orientations, the appearance of ambiguities is a sign that a method is conservative about the inferences it is willing to make. Discarding graphs with ambiguities entirely, therefore seems like an overly harsh punishment for a method not being willing to make strong claims. In Appendix D, we describe a procedure for computing best-case and worst-case distances to a ground truth for graphs with ambiguities by considering all possible ways in which ambiguities may be interpreted. The strategy is similar to the way in which the SID is defined for CPDAGs [Peters and Bühlmann, 2015, Section 2.4] as a pair of a worst- and best-case score across Markov equivalence class members.

#### 3.5 Analysing Robustness to Hyperparameter Changes

Another application of the s/c-distance besides validation against a ground truth in a simulated experiment, is to employ it as a metric for robustness of a causal discovery method against hyperparameter changes. If a method  $\mathcal M$  returns a valid output graph  $\mathcal G_1$  for the choice of hyperparameters  $\theta_1$  and a valid output graph  $\mathcal G_2$  for the choice of hyperparameters  $\theta_2$ , we can compute  $d_{s/c}(\mathcal G_1,\mathcal G_2)$  to determine how much the different outputs resemble each other in terms of their separations. Importantly, this comparison does not rely on the knowledge of a ground truth. As an example, we consider the stability of the DYNOTEARS [Zheng et al., 2018] algorithm on a real-world climate data set of three time-series describing monthly surface pressure anomalies in the West Pacific and monthly surface air temperature anomalies in the Central and East Pacific (780 months). The same dataset was analyzed in detail in [Runge et al., 2019] and is freely available at www.esrl.noaa.gov. DYNOTEARS has two regularization hyperparameters  $\lambda_a$  and  $\lambda_w$  as well as a maximal time lag  $\tau_{max}$  and threshold parameter  $w_{thresh}$ . For this example, we keep  $\lambda_w, \tau_{max}, w_{thresh}$  fixed at  $\lambda_w = 0.05, \tau_{max} = 5$  and  $w_{thresh} = 0.1$  and we only analyse how changes of  $\lambda_a$  affect the outcome in both s/c-distance and SHD in Figure 4. See Appendix F for a similar plot for the parameter  $\lambda_w$ . We stress that this is not meant to be an extensive analysis of DYNOTEARS, but rather an illustrative example of the role that the s/c-distance can play in robustness tests. The example also reproduces on real-world data the observation of Section 3.3 that small changes in SHD may correspond to large changes in s/c-distance.

# 3.6 Greedy Equivalent Search on the Sachs Dataset

As a second example, we apply  $Greedy\ Equivalence\ Search\ [Chickering, 2003]\ with the Gaussian BIC-score (implemented in the Python package <math>ges^5$ ) to the Sachs protein signaling dataset [Sachs et al., 2005]. We compute the s/c-, Markov, and Faithfulness distance and the SHD to the ground-truth graph that is provided by the Python package  $Causal\ Discovery\ Toolbox\ [Kalainathan\ and\ Goudet, 2019].$  We used  $1000\ randomly\ drawn\ statements\ per\ order\ k \ge 2$  and found an s/c-distance of 0.276, a Markov distance of 0.044, a Faithfulness distance of 0.93 and a normalized SHD of 0.31. The most remarkable of these outcomes is the weak performance of GES w.r.t. the Faithfulness distance. The GES-output only predicts about 7% of the separations that hold in the assumed ground truth graph correctly.

# 4 Error rates for CI-tests on Causal Graphs

Constraint-based causal discovery approaches, or at least those that are inspired by the PC-algorithm like FCI or PCMCI+, consist of three components: the conditional independence test  $(T, \alpha)$ , a sequential procedure that decides which triples  $(X, Y, \mathcal{S})$  to test based on previous decisions (the skeleton phase) and a set of rules to orient edges, see [Meek, 1995]. Due to the complicated error propagation in PC-like methods and the various sources of errors, it is often impossible to pinpoint what exactly went wrong if errors occur. However, if a ground truth graph  $\mathcal{G}_0$  is available, we can wonder how well the CI-test  $(T, \alpha)$  is able to see the separations/connections of  $\mathcal{G}_0$  in isolation and how a PC-like algorithm fares in comparison to that. As a baseline, we therefore define the following error rates for a CI-test  $(T, \alpha)$ .

<sup>&</sup>lt;sup>5</sup>https://github.com/juangamella/ges

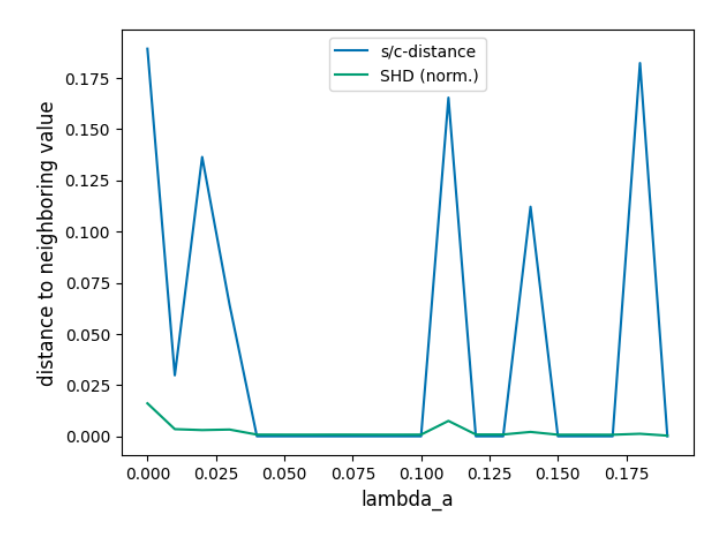


Figure 4: For each value of the regularization parameter  $\lambda_a$  of DYNOTEARS, we plot  $d_{s/c}(\mathcal{G}_{\lambda_a}, \mathcal{G}_{\lambda_a+0.005})$  and  $SHD(\mathcal{G}_{\lambda_a}, \mathcal{G}_{\lambda_a+0.005})$  to see how strongly the inferred graph changes when  $\lambda_a$  is increased. We see that the inferred graph is very stable in normalized SHD, but the changes in separations are much more significant. For instance, at  $\lambda_a = 0.11$ , about 16% of the implied separations/connections are affected. We believe that this effect is due to DYNOTEARS optimizing a score that considers two DAGs close to each other that have similar adjacency matrices. Thus, small hyperparameter changes only change few edges, but this does not provide a guarantee that separations remain similar.

Similarly to the indicator function that we used for causal graphs, for a CI-test  $(T, \alpha)$ , we define the separation indicator  $\iota_{(T,\alpha)}:\mathcal{C}\to\{0,1\}$  by

$$\iota_{(T,\alpha)}(X,Y,\mathcal{S}) = \begin{cases} 1 & \text{if } X \underline{\perp}_{(T,\alpha)} Y | \mathcal{S} \\ 0 & \text{else.} \end{cases}$$

**Definition 4.1.** Consider a causal graph  $\mathcal{G}_0$  with an appropriate notion of separation and let  $(T,\alpha)$  be a CI-test. We define

$$\begin{split} e^k_{s/c}(\mathcal{G}_0,(T,\alpha)) \\ := \frac{1}{|\mathcal{C}^k|} \sum_{(X,Y,\mathcal{S}) \in \mathcal{C}^k} |\iota_{\mathcal{G}_0}(X,Y,\mathcal{S}) - \iota_{(T,\alpha)}(X,Y,\mathcal{S})|. \end{split}$$

for  $k=0,\ldots,N-2$ . The **s/c-error rate up to order** K of  $(T,\alpha)$  is defined as  $e_{s/c}^{\leq K}(\mathcal{G}_0,\mathcal{G})=\frac{1}{K+1}\sum_{k=0}^K e_{s/c}^k(\mathcal{G}_0,\mathcal{G})$ . If K=N-2, we simply speak of the **s/c-error rate** and write  $e_{s/c}$  instead of  $e_{s/c}^{N-2}$ .

Once more, we can separate connections and separations in  $\mathcal{G}_0$  into false positive and false negative rates.

**Definition 4.2.** Consider a causal graph  $\mathcal{G}_0$  with an appropriate notion of separation, and let  $(T, \alpha)$  be a CI-test. We define

· We define

$$e_c^k(\mathcal{G}_0,(T,\alpha)) := \frac{1}{|\mathcal{C}_{con}^k(\mathcal{G}_0)|} \sum_{\substack{(X,Y,S) \\ \in \mathcal{C}_{con}^k(\mathcal{G}_0)}} \iota_{(T,\alpha)}(X,Y,\mathcal{S}).$$

for k = 0, ..., N - 2.

Then, we call  $e_c^{\leq K} = \frac{1}{K+1} \sum_{k=0}^K e_c^k(\mathcal{G}_0,\mathcal{G})$  the **c(onnection)-false negative rate up to order K** of the test  $(T,\alpha)$ . If K=N-2, we just speak of the **c-false negative rate** of the test  $(T,\alpha)$  and write  $e_c$  instead of  $e_c^{N-2}$ .

· We define

$$e_s^k(\mathcal{G}_0, (T, \alpha))$$

$$:= \frac{1}{|\mathcal{C}_{sep}^k(\mathcal{G}_0)|} \sum_{\substack{(X, Y, \mathcal{S}) \\ \in \mathcal{C}_{sep}^k(\mathcal{G}_0)}} 1 - \iota_{(T, \alpha)}(X, Y, \mathcal{S}).$$

for  $k=0,\ldots,N-2$ . Then, we call  $e_s^{\leq K}=\frac{1}{K+1}\sum_{k=0}^K e_s^k(\mathcal{G}_0,\mathcal{G})$  the **s(eparation)-false positive rate up to order K** of the test  $(T,\alpha)$ . If K=N-2, we just speak of the **s-false positive rate** of the test  $(T,\alpha)$  and write  $e_s$  instead of  $e_s^{N-2}$ .

As an averaged false positive rate, the s-false positive rate is controlled by  $\alpha$  provided that the distribution of the data is Markovian and faithful on  $\mathcal{G}_0$  and that the test's usual false positive rate is properly controlled by  $\alpha$ . The considerations regarding practical approximations of the s/c-distance in Section 3 also apply to the different types of test error rates of this section. The number of randomized conditional independence tests executed per order should be chosen depending on the running time of the statistical test and the availability of computational resources.

# Performance of the PC-algorithm with respect to Distance Measures

As an illustration of how to employ the introduced distance measures for empirical analyses against simulated data, we will ran a suite of experiments on the stable PC-algorithm [Spirtes et al., 1993, Colombo and Maathuis, 2014] with the partial correlation conditional independence test, and computed distances to the ground truth graph as well as error rates for the CI-test and conflict rates. We ran stable PC-ParCorr on data that was from linear additive SCMs matching the PC-algorithms assumptions as well as on data data that was generated from SCMs with non-linear components, violation the linearity assumption of the partial correlation test, and we investigated performance on different sample sizes (between 50 and 10000) and number of variables N = 5, 8, 12 and for different values of the significance level  $\alpha$  of the partial correlation test ( $\alpha = 0.01$  and  $\alpha = 0.05$ ). We ran 100 randomized experiments for each parameter combination. Details on the data generation and detailed figures can be found in Appendix C. The main takeaways of our experiments are the following:

- (1) The Markov distance of the PC-algorithm's valid outputs matches the c-false negative rate for small and medium sample sizes and improves on it for large sample sizes if the data generation conforms to PC's assumptions. Similarly, the s/c-distance roughly matches the s/c-error rate of the ParCorr test in this setting. For 12 variables, the Markov distance to the ground truth was still above 0.1 for 1000 samples and at about 0.04 for 10000 samples with a test significance of  $\alpha = 0.05$ . This might indicate that, even on favorable data, good inferences w.r.t. Markov distance require large samples.
- (2) The Faithfulness distance of the PC-algorithm's valid outputs is larger than the s-false positive rate for small sample sizes and larger graphs and does not seem to be controlled by the significance level of the test.

# Conclusion

We have introduced new quantities for evaluating causal discovery methods against simulated data that measure how accurately a given method infers the Markov equivalence class of the ground truth graph. While the primary purpose of this work was to introduce the new distance measures as a tool for causal discovery researchers to evaluate newly introduced methods, a thorough analysis of existing causal discovery algorithms against these metrics, or an extensive hyperparameter sensitivity analysis of causal discovery on real-world data would be interesting projects for future research. In particular, it would be interesting to see how sensitive score-based approaches to causal discovery are to changes of hyperparameters w.r.t. separation statements.

Acknowledgements JW and JR received funding from the European Research Council (ERC) Starting Grant CausalEarth under the European Union's Horizon 2020 research and innovation program (Grant Agreement No. 948112). We thank Christopher Lohse for sharing his implementation of the DYNOTEARS algorithm and Simon Bing for proof-reading a previous version of this manuscript.

Author Contributions JR pointed out the need to compare causal graphs in climate-related applications. JW conceived the project, wrote the manuscript and carried out the experiments. JR advised JW on dealing with orientation conflicts/ambiguous triples, and on the use of the Tigramite software package. JR also pointed JW to several important references and related works, and shared code for generating simulated data with JW.

## References

- S. Acid and L. M. d. Campos. Searching for Bayesian Network Structures in the Space of Restricted Acyclic Partially Directed Graphs. *Journal of Artificial Intelligence Research*, 18:445–490, 2003.
- K. Biza, I. Tsamardinos, and S. Triantafillou. Tuning Causal Discovery Algorithms. In *Proceedings of the 10th International Conference on Probabilistic Graphical Models*, pages 17–28. PMLR, 2020.
- S. Bongers, P. Forré, J. Peters, and J. M. Mooij. Foundations of structural causal models with cycles and latent variables. *The Annals of Statistics*, 49(5):2885–2915, 2021. Publisher: Institute of Mathematical Statistics.
- D. M. Chickering. Optimal structure identification with greedy search. *The Journal of Machine Learning Research*, 3: 507–554, 2003.
- T. Claassen and T. Heskes. A Bayesian approach to constraint based causal inference. In *Proceedings of the Twenty-Eighth Conference on Uncertainty in Artificial Intelligence*, UAI'12, pages 207–216, Arlington, Virginia, USA, 2012. AUAI Press.
- D. Colombo and M. H. Maathuis. Order-Independent Constraint-Based Causal Structure Learning. *Journal of Machine Learning Research*, 15(116):3921–3962, 2014.
- E. Eulig, A. A. Mastakouri, P. Blöbaum, M. Hardt, and D. Janzing. Toward Falsifying Causal Graphs Using a Permutation-Based Test, 2023. arXiv:2305.09565 [cs, stat].
- P. M. Faller, L. C. Vankadara, A. A. Mastakouri, F. Locatello, and D. Janzing. Self-Compatibility: Evaluating Causal Discovery without Ground Truth, 2023. arXiv:2307.09552 [cs, stat].
- A. Gerhardus and J. Runge. High-recall causal discovery for autocorrelated time series with latent confounders. In *Advances in Neural Information Processing Systems*, volume 33, pages 12615–12625. Curran Associates, Inc., 2020.
- L. Henckel, T. Würtzen, and S. Weichwald. Adjustment identification distance: A gadget for causal structure learning, 2024. arXiv:2402.08616 [ML].
- A. Hyttinen, F. Eberhardt, and M. Järvisalo. Constraint-based causal discovery: Conflict resolution with answer set programming. In *UAI*, pages 340–349, 2014.
- D. Kalainathan and O. Goudet. Causal discovery toolbox: Uncover causal relationships in python, 2019. arXiv:1903.02278 [stats].
- M. Kocaoglu. Characterization and learning of causal graphs with small conditioning sets. In *Thirty-seventh Conference on Neural Information Processing Systems*, 2023.
- H. Li, V. Cabeli, N. Sella, and H. Isambert. Constraint-based causal structure learning with consistent separating sets. In *Advances in Neural Information Processing Systems*, volume 32. Curran Associates, Inc., 2019.
- H. Liu, K. Roeder, and L. Wasserman. Stability approach to regularization selection (stars) for high dimensional graphical models. In Advances in Neural Information Processing Systems, volume 23. Curran Associates, Inc., 2010.
- D. Machlanski, S. Samothrakis, and P. Clarke. Robustness of Algorithms for Causal Structure Learning to Hyperparameter Choice, 2023. arXiv:2310.18212 [cs. stat].
- C. Meek. Causal inference and causal explanation with background knowledge. In *Proceedings of the Eleventh conference on Uncertainty in artificial intelligence*, UAI'95, pages 403–410, San Francisco, CA, USA, 1995.
- O. A. Mian, A. Marx, and J. Vreeken. Discovering Fully Oriented Causal Networks. *Proceedings of the AAAI Conference on Artificial Intelligence*, 35(10):8975–8982, 2021.
- H. Parikh, C. Varjao, L. Xu, and E. T. Tchetgen. Validating Causal Inference Methods. In *Proceedings of the 39th International Conference on Machine Learning*, pages 17346–17358. PMLR, 2022.
- J. Peters and P. Bühlmann. Structural intervention distance for evaluating causal graphs. *Neural computation*, 27(3): 771–799, 2015. Publisher: MIT Press.
- J. Pitchforth and K. Mengersen. A proposed validation framework for expert elicited Bayesian Networks. *Expert Systems with Applications*, 40(1):162–167, 2013.
- J. Ramsey, P. Spirtes, and J. Zhang. Adjacency-faithfulness and conservative causal inference. In *Proceedings of the Twenty-Second Conference on Uncertainty in Artificial Intelligence*, UAI'06, pages 401–408. AUAI Press, 2006.

- A. Reisach, C. Seiler, and S. Weichwald. Beware of the Simulated DAG! Causal Discovery Benchmarks May Be Easy to Game. In *Advances in Neural Information Processing Systems*, volume 34, pages 27772–27784. Curran Associates, Inc., 2021.
- A. G. Reisach, M. Tami, C. Seiler, A. Chambaz, and S. Weichwald. A scale-invariant sorting criterion to find a causal order in additive noise models. In *Thirty-seventh Conference on Neural Information Processing Systems*, 2023.
- J. Runge. Discovering contemporaneous and lagged causal relations in autocorrelated nonlinear time series datasets. In *Proceedings of the 36th Conference on Uncertainty in Artificial Intelligence (UAI)*, pages 1388–1397. PMLR, 2020.
- J. Runge, P. Nowack, M. Kretschmer, S. Flaxman, and D. Sejdinovic. Detecting and quantifying causal associations in large nonlinear time series datasets. *Science Advances*, 5(11), Nov. 2019. Publisher: American Association for the Advancement of Science.
- K. Sachs, O. Perez, D. Pe'er, D. A. Lauffenburger, and G. P. Nolan. Causal protein-signaling networks derived from multiparameter single-cell data. *Science*, 308(5721):523–529, 2005.
- S. Shimizu, P. O. Hoyer, A. Hyvärinen, A. Kerminen, and M. Jordan. A linear non-Gaussian acyclic model for causal discovery. *Journal of Machine Learning Research*, 7(10), 2006.
- P. Spirtes, C. Glymour, and R. Scheines. *Causation, Prediction, and Search*, volume 81 of *Lecture Notes in Statistics*. Springer, New York, NY, 1993.
- P. L. Spirtes, C. Meek, and T. S. Richardson. Causal Inference in the Presence of Latent Variables and Selection Bias, 2013. arXiv:1302.4983 [cs].
- J. Textor, B. van der Zander, M. S. Gilthorpe, M. Liskiewicz, and G. T. Ellison. Robust causal inference using directed acyclic graphs: the R package 'dagitty'. *International Journal of Epidemiology*, 45(6):1887–1894, 2016.
- I. Tsamardinos, L. E. Brown, and C. F. Aliferis. The max-min hill-climbing Bayesian network structure learning algorithm. *Machine Learning*, 65(1):31–78, 2006.
- J. Zhang. Causal reasoning with ancestral graphs. Journal of Machine Learning Research, 9:1437–1474, 2008.
- X. Zheng, B. Aragam, P. K. Ravikumar, and E. P. Xing. DAGs with NO TEARS: Continuous Optimization for Structure Learning. In *Advances in Neural Information Processing Systems*, volume 31. Curran Associates, Inc., 2018.

# **Appendix A** Definitions of SHD and SID

Here, we will recall the formal definitions of SHD and SID where we restrict ourselves to DAGs.

**Definition A.1** (Acid and Campos [2003], Tsamardinos et al. [2006]). The structural Hamming distance  $SHD(\mathcal{G}, \mathcal{H})$  between two DAGs  $\mathcal{G}$  and  $\mathcal{H}$  over the set of nodes  $\mathbf{X}$  is defined as

$$SHD(\mathcal{G}, \mathcal{H}) = |\{(X, Y) \in \mathbf{X} \times \mathbf{X}, X \neq Y, | \mathcal{G} \text{ and } \mathcal{H} \text{ do not have the same type of edge between } X \text{ and } Y\}|.$$

To keep matters simple, for the SID we do not use its original definition [Peters and Bühlmann, 2015, Definition 4] but its equivalent graphical characterization [Peters and Bühlmann, 2015, Proposition 6] . For a DAG  $\mathcal G$  over  $\mathbf X$  with nodes X,Y and  $\mathcal S\subset \mathbf X\setminus\{X,Y\}$ , [Peters and Bühlmann, 2015] defined the following property (\*) of  $\mathcal C$  w.r.t.  $(\mathcal G,X,Y)$ :

In  $\mathcal{G}$ , no  $S \in \mathcal{S}$  is a descendant of any W which lies on a directed path from X to Y and  $\mathcal{S}$  blocks all non-directed paths from X to Y.

**Definition A.2** (Peters and Bühlmann [2015]). The structural intervention distance (SID)  $SID(\mathcal{G}, \mathcal{H})$  between two DAGs  $\mathcal{G}$  and  $\mathcal{H}$  over the set of nodes  $\mathbf{X}$  is given by

$$\mathrm{SID}(\mathcal{G},\mathcal{H}) = \left| \left. \left\{ (X,Y) \in \mathbf{X} \times \mathbf{X}, \ X \neq Y, \ \middle| \begin{matrix} Y \in \mathrm{pa}_{\mathcal{H}}(X) \text{ and } Y \in \mathrm{de}_{\mathcal{G}}(X) & \text{or} \\ Y \notin \mathrm{pa}_{\mathcal{H}}(X) \text{ and } \mathrm{pa}_{\mathcal{H}}(X) \text{ does not satisfy } (*) \text{ for } (\mathcal{G},X,Y) \end{matrix} \right\} \right|$$

where  $pa_{(\cdot)}(\cdot)$  and  $de_{(\cdot)}(\cdot)$  refer to parents and descendants in the respective graphs.

# Appendix B Proofs

We prove the following Lemma of which 3.2 is a special case (K = N - 2).

**Lemma B.1.** Let  $\mathbb{G}$  be a class of graphs with an appropriate notion of separation, e.g.  $\mathbb{G} = \{MAGs\}$  and m-separation.  $d_{s/c}^{\leq K}$  is a metric on the set  $\mathbb{G}/\sim$  of K-th order Markov equivalence classes of  $\mathbb{G}$ .

*Proof.* Consider the real vector space  $V_k$  of maps  $\mathcal{C}_k \to \mathbb{R}$  on which  $\|f\|_k = \frac{1}{\mathcal{C}_k} \sum_{(X,Y,\mathcal{S}) \in \mathcal{C}_k} |f_k(X,Y,\mathcal{S})|$  defines a norm. Then  $\|(f_0,\ldots,f_K)\| := \sum_{k=0}^K \|f_k\|_k$  defines a norm on the graded vector space  $V_K = \bigoplus_{k=0}^K V_k$ . We now define the mapping

$$g_K: \mathbb{G} \to V_K, \qquad \mathcal{G} \mapsto (i_{\mathcal{G}}|_{\mathcal{C}_0}, \dots, i_{\mathcal{G}}|_{\mathcal{C}_K}),$$

where  $i_{\mathcal{G}}|_{\mathcal{C}_k}$  is the separation indication function restricted to the set of k-th order separation/connection statements. We observe that  $g_K(\mathcal{G}_0) = g_K(\mathcal{G})$  if and only if  $\mathcal{G}_0$  and  $\mathcal{G}$  have the same separations up to order K. In other words, the mapping  $g_K$  is well-defined on the quotient f of f-th order Markov equivalence classes and becomes an embedding. Since  $d_{s/c}^{\leq K}(\mathcal{G}_0,\mathcal{G})$  is nothing but

$$d_{s/c}^{\leq K}(\mathcal{G}_0, \mathcal{G}) = \|g_K(\mathcal{G}_0) - g_K(\mathcal{G})\|,$$

it follows directly that  $d_{s/c}^{\leq K}(\mathcal{G}_0,\mathcal{G})$  is a metric on  $\mathbb{G}_{\sim}$ . Finally, since the usual notion of Markov equivalence means that two graphs share exactly the same separations,  $\mathcal{G}_0$  and  $\mathcal{G}$  are Markov equivalent if and only if  $d_{s/c}(\mathcal{G}_0,\mathcal{G})=d_{s/c}^{\leq N-2}(\mathcal{G}_0,\mathcal{G})=0$ , so this is indeed the special case where K=N-2 by which point all separation statements have been exhausted.

*Proof of Lemma 3.5.* If  $d_c(\mathcal{G}_0,\mathcal{G}) \neq 0$ , then there must be a triple  $(X,Y,\mathcal{S}) \in \mathcal{C}_{con}(\mathcal{G}_0) \cap \mathcal{C}_{sep}(\mathcal{G})$ . Since  $(X,Y,\mathcal{S}) \in \mathcal{C}_{con}(\mathcal{G}_0)$  and  $P_{\mathbf{X}}$  is faithful on  $\mathcal{G}_0$ , we must have that  $X \not\perp_{P_{\mathbf{X}}} Y | \mathcal{S}$ . If  $P_{\mathbf{X}}$  would be Markovian on  $\mathcal{G}$ ,  $(X,Y,\mathcal{S}) \in \mathcal{C}_{sep}(\mathcal{G})$  would imply  $X \perp_{P_{\mathbf{X}}} Y | \mathcal{S}$ , which is a contradiction. Conversely, if  $P_{\mathbf{X}}$  is not Markovian on  $\mathcal{G}$ , there must be a triple  $(X,Y,\mathcal{S}) \in \mathcal{C}_{sep}(\mathcal{G})$  with  $X \not\perp_{P_{\mathbf{X}}} Y | \mathcal{S}$ . Since  $P_{\mathbf{X}}$  is Markovian on  $\mathcal{G}_0$ , it follows that  $(X,Y,\mathcal{S}) \in \mathcal{C}_{con}(\mathcal{G}_0) \cap \mathcal{C}_{sep}(\mathcal{G})$ . Hence  $d_c(\mathcal{G}_0,\mathcal{G}) \neq 0$ . □

*Proof of Lemma 3.7.* If  $d_s(\mathcal{G}_0,\mathcal{G}) \neq 0$ , then there must be a triple  $(X,Y,\mathcal{S}) \in \mathcal{C}_{sep}(\mathcal{G}_0) \cap \mathcal{C}_{con}(\mathcal{G})$ . Since  $(X,Y,\mathcal{S}) \in \mathcal{C}_{sep}(\mathcal{G}_0)$  and  $P_{\mathbf{X}}$  is Markovian on  $\mathcal{G}_0$ , we must have that  $X \perp\!\!\!\perp_{P_{\mathbf{X}}} Y | \mathcal{S}$ . If  $P_{\mathbf{X}}$  would be faithful on  $\mathcal{G}$ ,  $(X,Y,\mathcal{S}) \in \mathcal{C}_{con}(\mathcal{G})$  would imply  $X \perp\!\!\!\perp_{P_{\mathbf{X}}} Y | \mathcal{S}$ , which is a contradiction. Conversely, if  $P_{\mathbf{X}}$  is not faithful on  $\mathcal{G}$ , there must a triple  $(X,Y,\mathcal{S}) \in \mathcal{C}_{con}(\mathcal{G})$  with  $X \perp\!\!\!\perp_{P_{\mathbf{X}}} Y | \mathcal{S}$ . Since  $P_{\mathbf{X}}$  is faithful on  $\mathcal{G}_0$ , it follows that  $(X,Y,\mathcal{S}) \in \mathcal{C}_{sep}(\mathcal{G}_0)$  and thus  $(X,Y,\mathcal{S}) \in \mathcal{C}_{sep}(\mathcal{G}_0) \cap \mathcal{C}_{con}(\mathcal{G})$ . But this means that  $d_s(\mathcal{G}_0,\mathcal{G}) \neq 0$ . □

# Appendix C Empirical Analysis of the PC-algorithm

In this section, we present several plots describing the performance of the stable PC-algorithm with the partial correlation CI-test on simulated data with respect to the distance metrics introduced in this work. Data was generated from additive structural causal models of the form  $X_i = f_i(\operatorname{pa}(X_i)) + \eta_i$  over randomly drawn DAGs. The noise variables are centered Gaussians with variances drawn uniformly at random between 0.2 and 2.0. In the first suite of experiments, the SCMs are assumed additive and the mechanisms  $f_i$  are assumed linear with effect strengths drawn uniformly at random between 0.1 and 1.0. In the second suite of experiments, the mechanisms are multiplicative functions  $f_i = \lambda_i \prod_{X_j \in \operatorname{pa}(X_i)} X_j$  with  $\lambda \in [0.1, 1]$ . Experimental parameters include the number of variables (N = 5, 8, 12), the significance level of the test  $(\alpha = 0.01, 0.05)$  and the sample sizes (between 50 and 10000 depending on the experiment). For each parameter configuration 100 experiments are run.

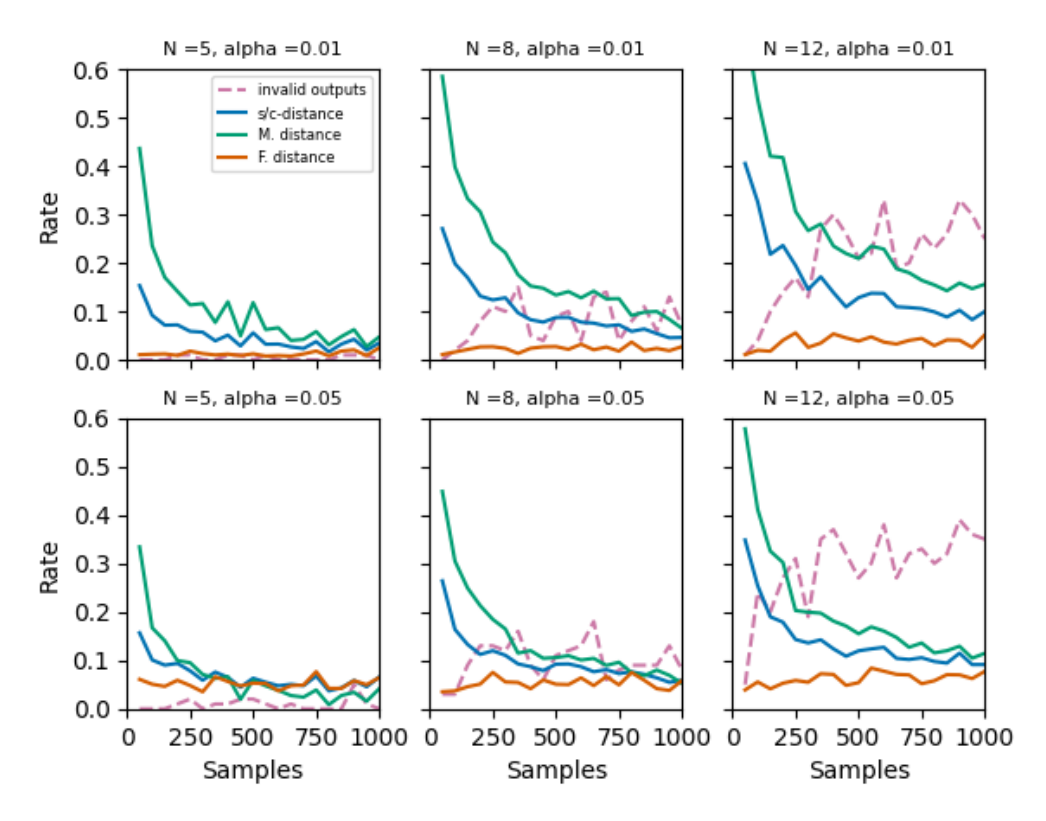


Figure 5: Distances of the output of the stable PC-algorithm (ParCorr) to the ground truth DAG across 100 experiments on data generated from linear additive models. Markov, Faithfulness and s/c-distance are only computed on valid output graphs. For 12 variables, Markov and s/c-distance are still quite high even for 1000 available samples, indicating that higher sample sizes are needed for sufficently reliable inferences on this data.

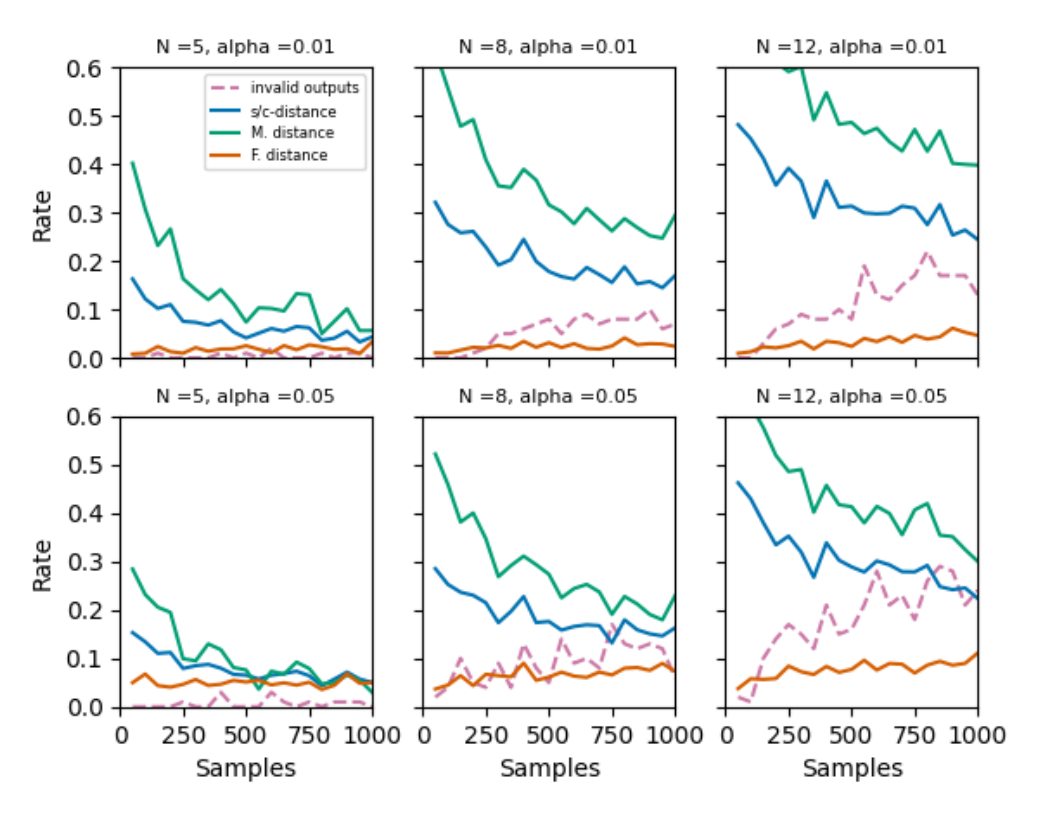


Figure 6: Distances of the output of the stable PC-algorithm (ParCorr) to the ground truth DAG across 100 experiments on data generated from additive models with nonlinear mechanism functions. The linearity assumptions needed for the partial correlation CI-test are violated which manifests in clearly elevated distance rates at all variable sizes.

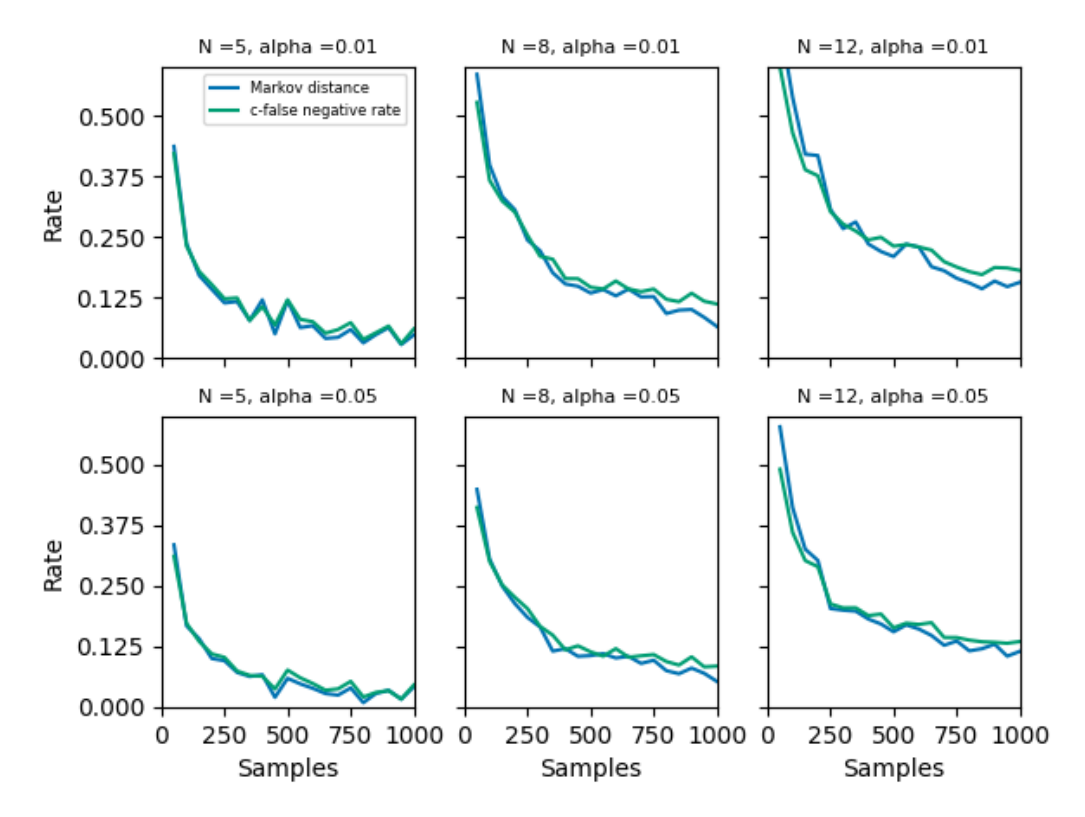


Figure 7: Comparison of Markov distance of the output of the stable PC-algorithm (ParCorr) to the ground truth DAG and the c-false negative rate of the ParCorr test by itself across 100 experiments on data generated from linear additive models. Invalid output graphs were disregarded. At this range of sample sizes (up to 1000 samples per experiment), the Markov distances largely tracks the c-false negative rate and a significant improvement is only seen at higher sample sizes, see Figure 8.

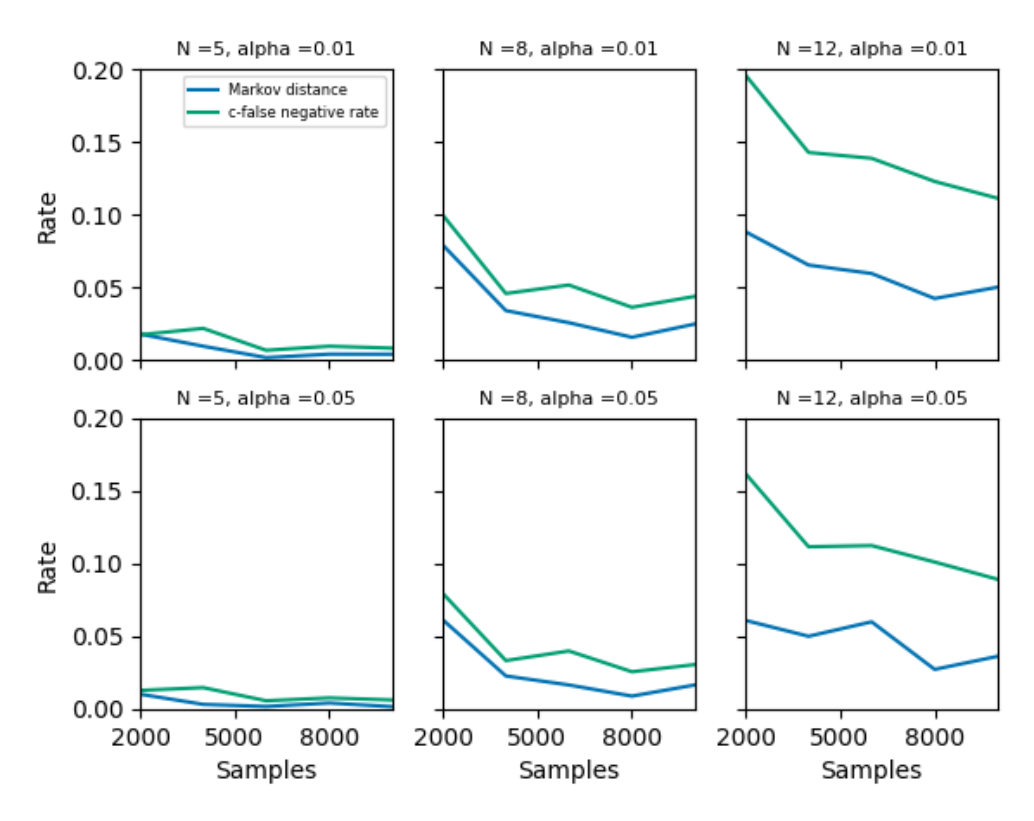


Figure 8: Comparison of Markov distance of the output of the stable PC-algorithm (ParCorr) to the ground truth DAG and the c-false negative rate of the ParCorr test by itself across 100 experiments on data generated from linear additive models. Invalid output graphs were disregarded. Beyond sample sizes of 2000 samples per experiments, the Markov distance of the PC-output is closer to zero than the c-false negative rate.

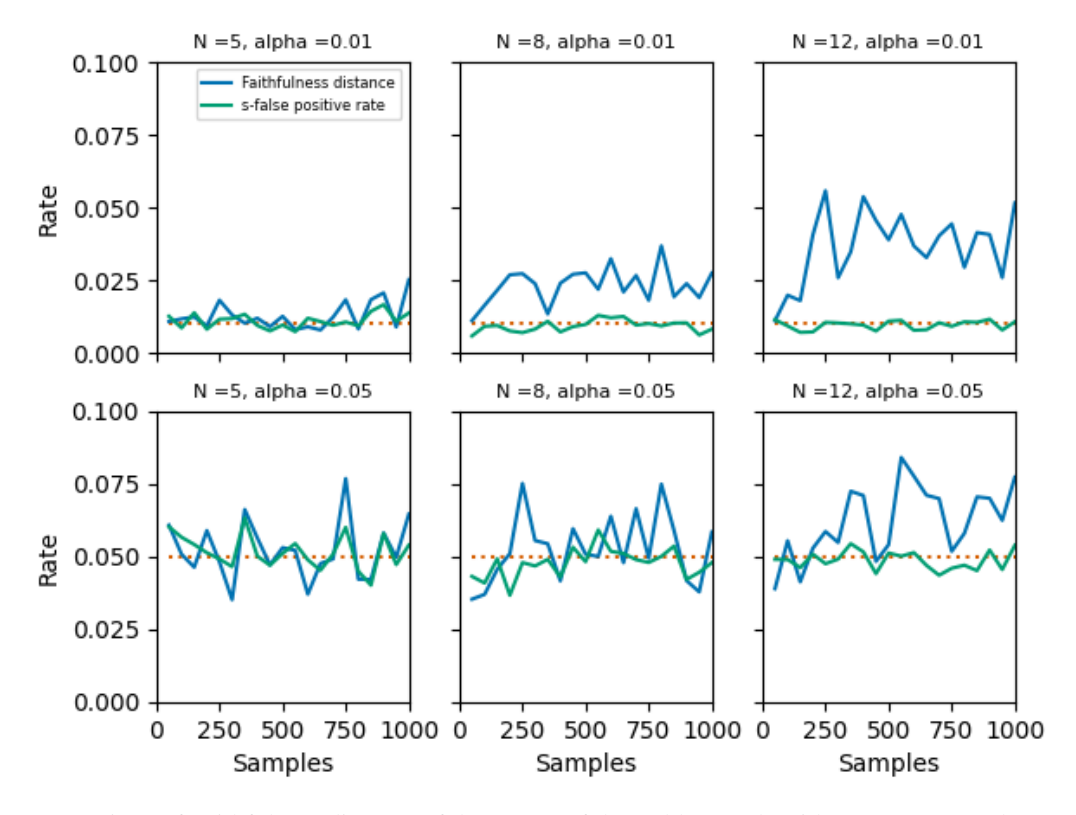


Figure 9: Comparison of Faithfulness distance of the output of the stable PC-algorithm (ParCorr) to the ground truth DAG and the s-false positive rate of the ParCorr test by itself across 100 experiments on data generated from linear additive models. Invalid output graphs were disregarded. The s-false positive rate is controlled at level  $\alpha$  while the Faithfulness distance is higher at sample sizes up to 1000 samples per experiment.

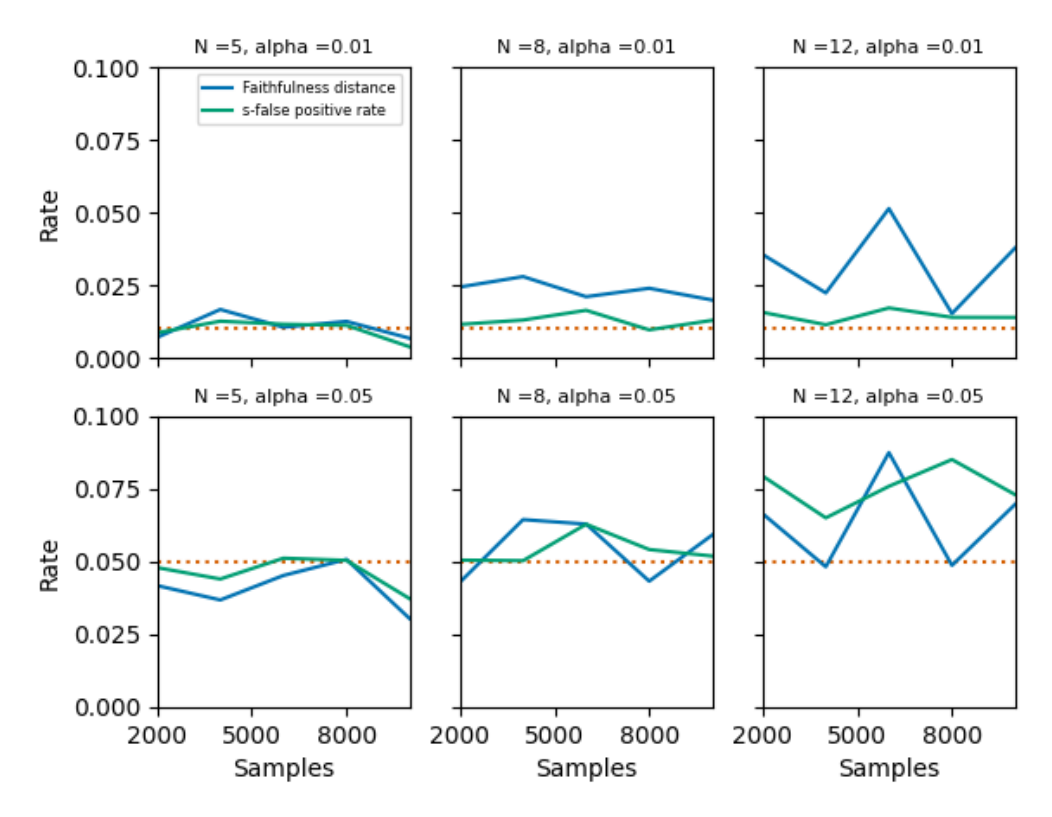


Figure 10: Comparison of Faithfulness distance of the output of the stable PC-algorithm (ParCorr) to the ground truth DAG and the s-false positive rate of the ParCorr test by itself across 100 experiments on data generated from linear additive models. Invalid output graphs were disregarded. For 8 and 12 variables, the s-FPR is no longer concrolled indicating that there might have been a relevant amount of Faithfulness violations in our data generation scheme, perhaps due to cancellations of effects along different paths.

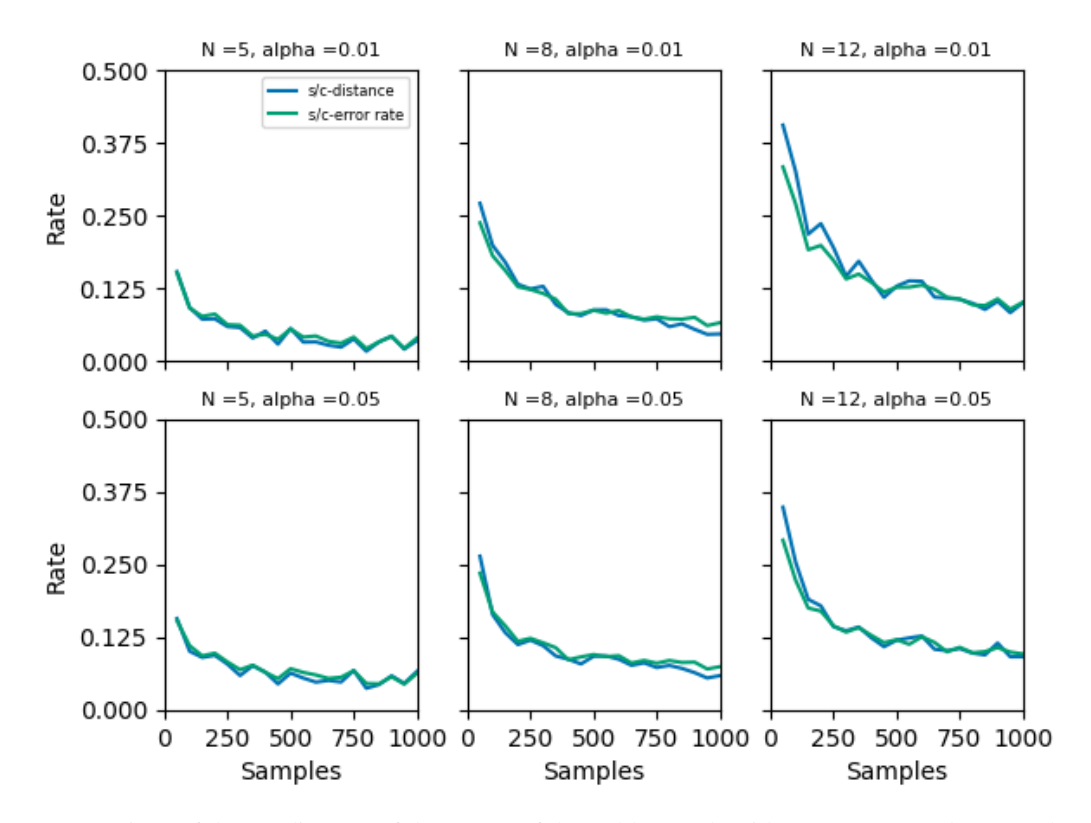


Figure 11: Comparison of the s/c-distance of the output of the stable PC-algorithm (ParCorr) to the ground truth DAG and the s/c-error rate of the ParCorr test by itself across 100 experiments on data generated from linear additive models. Invalid output graphs were disregarded. At sample sizes up to 1000 samples per experiment, both quantities are virtually the same in our experiments.

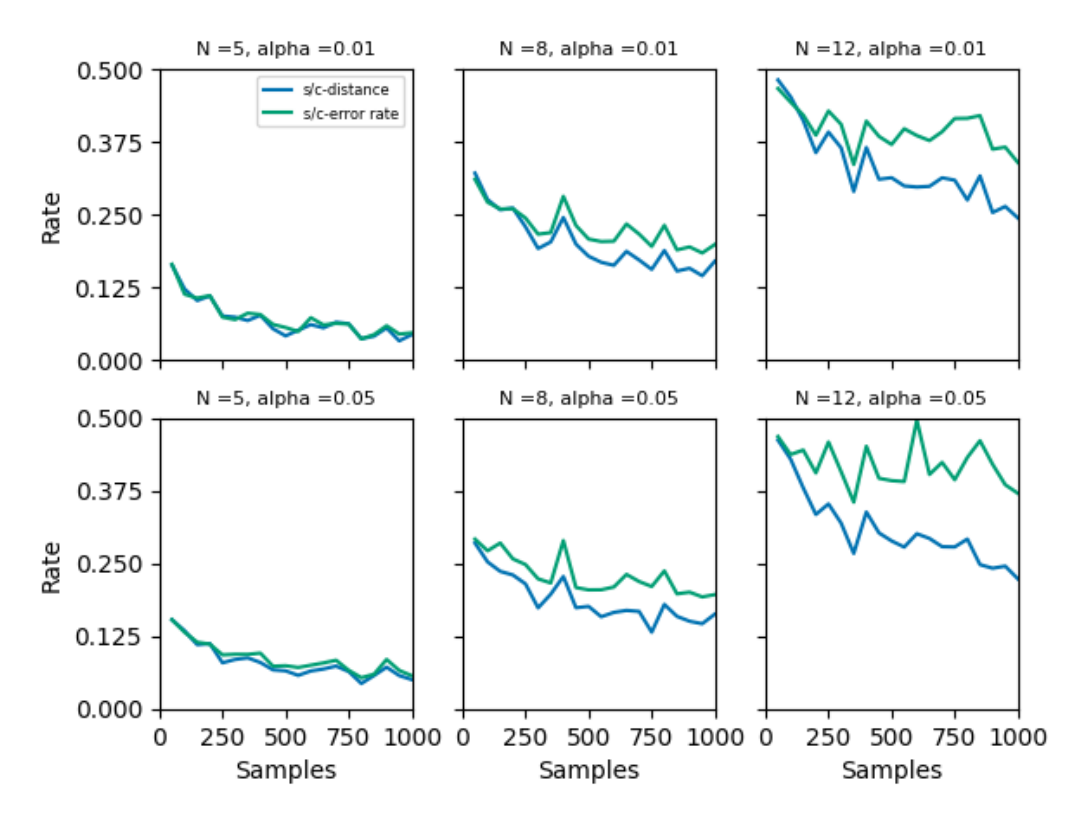


Figure 12: Comparison of the s/c-distance of the output of the stable PC-algorithm (ParCorr) to the ground truth DAG and the s/c-error rate of the ParCorr test by itself across 100 experiments on data generated from nonlinear additive models. Invalid output graphs were disregarded. Performance is significantly impaired in comparison to the linear setting of Figure 11.

# **Appendix D** Computing Distances for Graphs with Ambiguities

In this section, we propose a method to compute best-case and worst-case estimate for directed acyclic graphs with ambiguous unshielded triples from which separation and connection statements cannot be straightforwardly computed. The proposed strategy is similar to how the structural intervention distance is computed for CPDAG by iterating through all DAGs that are represented by a given CPDAG, see [Peters and Bühlmann, 2015]. Recall that a triple of nodes (X,Y,Z) on a directed or undirected graph  $\mathcal G$  is unshielded if X and Y are neighbors on  $\mathcal G$ , Y and Z are neighbors on  $\mathcal G$  but X and Z are not neighbors on  $\mathcal G$ . The procedure will start with the following input data:

- A (ground truth) DAG or CPDAG  $\mathcal{G}_0$ ;
- An undirected graph  $\mathcal{G}$  that will serve as the skeleton of a DAG or tsDAG;
- A partition of the set of unshielded triples  $\mathcal{U} = \mathcal{U}_c \cup \mathcal{U}_{nc} \cup \mathcal{U}_a$  into colliders  $(\mathcal{U}_c)$ , non-colliders  $(\mathcal{U}_{nc})$  and ambiguous triples  $(\mathcal{U}_a)$ .
- An indicator  $x \in \{s/c, c, s\}$  to specify which distance to compute.

This information is part of the output of the conservative PC algorithm [Ramsey et al., 2006], the stable PC algorithm with the majority rule [Colombo and Maathuis, 2014] or the Tigramite implementation of PCMCI+ with the conservative or majority contemporary collider rule [Runge, 2020].

From this input, we now generate a list of CPDAGs  $(\mathcal{G}_{\mathcal{B}})$  where  $\mathcal{B} \subset \mathcal{U}_a$ . For each CPDAG  $\mathcal{G}_{\mathcal{B}}$  in this list, we then compute  $d_x(\mathcal{G}_0, \mathcal{G}_{\mathcal{B}})$  and, finally, we arrive at the best-case, average and worst-case estimate

$$\min_{\mathcal{B} \subset \mathcal{U}_a} d_x(\mathcal{G}_0, \mathcal{G}_{\mathcal{B}}), \qquad \operatorname{mean}(d_x(\mathcal{G}_0, \mathcal{G}_{\mathcal{B}})) \qquad \max_{\mathcal{B} \subset \mathcal{U}_a} d_x(\mathcal{G}_0, \mathcal{G}_{\mathcal{B}}).$$

The details are outlined as pseudocode in Algorithm 1 below.

# Algorithm 1 Pseudocode to compute distance measures for graphical outputs with ambiguities.

**Require:**  $\mathcal{G}_0$ ,  $\mathcal{G}$ ,  $\mathcal{U}_c$ ,  $\mathcal{U}_a$  as defined above. Indicator  $x \in \{s/c, c, s\}$  to specify distance measure.

```
Initialize empty list \mathcal{L}.
for all \mathcal{B} \subset \mathcal{U}_a do
     \mathcal{G}_{\mathcal{B}} \leftarrow \mathcal{G};
     COL \leftarrow \mathcal{U}_c \cup \mathcal{B};
     Collider phase: try: orient all (X, Y, Z) \in COL as colliders on \mathcal{G}_{\mathcal{B}};
     if No conflicting orientations and no cycle in \mathcal{G}_{\mathcal{B}} then
         Orientation phase: try: Apply Meek's orientation rules to \mathcal{G}_{\mathcal{B}};
         if No conflicting orientations and no cycle in \mathcal{G}_{\mathcal{B}} then
              append \mathcal{G}_{\mathcal{B}} to \mathcal{L};
         end if
     end if
end for
if \mathcal{L} = \emptyset then
     max-dist, mean-dist, min-dist \leftarrow 1;
     \max - \operatorname{dist} \leftarrow \max_{\mathcal{B} \in \mathcal{L}} d_x(\mathcal{G}_0, \mathcal{G}_{\mathcal{B}});
     mean-dist \leftarrow \operatorname{mean}_{\mathcal{B} \in \mathcal{L}} d_x(\mathcal{G}_0, \mathcal{G}_{\mathcal{B}});
    \min-\text{dist} \leftarrow \min_{\mathcal{B} \in \mathcal{L}} d_x(\mathcal{G}_0, \mathcal{G}_{\mathcal{B}});
end if
return max-dist, mean-dist, min-dist.
```

# **Appendix E Pseudocode for Computing Distance Metrics**

In this section, we provide pseudocode to compute the distance and obscurity measures introduced in the main document. All of these measures rely on an oracle function  $\operatorname{Oracle}_{\mathcal{G}}(X,Y,\mathcal{S})$  that takes in a causal graph and a triple  $(X,Y,\mathcal{S}) \in \mathcal{C}$  and outputs 1 if X and Y are separated and 0 if they are connected by  $\mathcal{S}$  in  $\mathcal{G}$ . Practical implementations of such an oracle for DAGs (d-separation) are available in the R package Dagitty [Textor et al., 2016] and the Python package Tigramite (https://github.com/jakobrunge/tigramite). The oracle implemented in Tigramite is also applicable to MAGs (m-separation), tsMAGs and tsDAGs.

# Algorithm 2 Pseudocode to compute the s/c-distance.

```
Require: \mathcal{G}_0, \mathcal{G} causal graphs (e.g. DAGs) or Markov equivalence classes (e.g. CPDAGs) with N nodes, Oracle for
    fitting notion of separation. Sets \mathcal{L}_k of order k-triples to be tested for k=0,\ldots,N-2.
    if \mathcal{G}_0 (or \mathcal{G}) is Markov equivalence class then
       \mathcal{G}_0 (or \mathcal{G}) \leftarrow member of \mathcal{G}_0 (or \mathcal{G});
    end if
    dist = 0.0;
    for k=0,\ldots,N-2 do
       dist_k = 0.0;
       count = 0;
       for triples (X, Y, S) \in \mathcal{L}_k do
           count += 1;
           \operatorname{dist}_k += |\operatorname{Oracle}_{\mathcal{G}_0}(X, Y, \mathcal{S}) - \operatorname{Oracle}_{\mathcal{G}}(X, Y, \mathcal{S})|;
       end for
       \operatorname{dist} += \frac{\operatorname{dist}_k}{\operatorname{count}};
    end for
   return \frac{\text{dist}}{N-1}.
```

## **Algorithm 3** Pseudocode to compute the Markov distance (c-distance).

```
Require: \mathcal{G}_0, \mathcal{G} causal graphs (e.g. DAGs) or Markov equivalence classes (e.g. CPDAGs) with N nodes, Oracle for
   fitting notion of separation. Sets \mathcal{L}_k of order k-triples to be tested for k=0,\ldots,N-2.
   if \mathcal{G}_0 (or \mathcal{G}) is Markov equivalence class then
       \mathcal{G}_0 (or \mathcal{G}) \leftarrow member of \mathcal{G}_0 (or \mathcal{G});
   end if
   dist = 0.0;
   for k = 0, ..., N - 2 do
       dist_k = 0.0;
       count = 0;
       for triples (X,Y,\mathcal{S})\in\mathcal{L}_k do
           if \operatorname{Oracle}_{\mathcal{G}_0}(X,Y,\mathcal{S}) == 0 then
              count += 1;
              if \operatorname{Oracle}_{\mathcal{G}}(X,Y,\mathcal{S}) == 1 then
                  \operatorname{dist}_k += 1;
               end if
          end if
       end for
       \operatorname{dist} += \frac{\operatorname{dist}_k}{\operatorname{count}};
   end for
   return \frac{\text{dist}}{N-1}.
```

## **Algorithm 4** Pseudocode to compute the Faithfulness distance (s-distance).

```
Require: \mathcal{G}_0, \mathcal{G} causal graphs (e.g. DAGs) or Markov equivalence classes (e.g. CPDAGs) with N nodes, Oracle for
   fitting notion of separation. Sets \mathcal{L}_k of order k-triples to be tested for k=0,\ldots,N-2.
   if \mathcal{G}_0 (or \mathcal{G}) is Markov equivalence class then
       \mathcal{G}_0 (or \mathcal{G}) \leftarrow member of \mathcal{G}_0 (or \mathcal{G});
   end if
   dist = 0.0;
   for k=0,\ldots,N-2 do
       dist_k = 0.0;
       count = 0;
       for triples (X, Y, S) \in \mathcal{L}_k do
          if \operatorname{Oracle}_{\mathcal{G}_0}(X,Y,\mathcal{S}) == 1 then
              count += 1;
              if Oracle_{\mathcal{G}}(X, Y, \mathcal{S}) == 0 then
                  \operatorname{dist}_k += 1;
              end if
          end if
       end for
       \operatorname{dist} += \frac{\operatorname{dist}_k}{\operatorname{count}};
   end for
   return \frac{\text{dist}}{N-1}.
```

## **Algorithm 5** Pseudocode to compute s/c-obscurity.

**Require:** Causal graph  $\mathcal{G}_0$  (e.g. DAG) or Markov equivalence class (e.g. CPDAG) with N nodes, Oracle for fitting notion of separation. Sets  $\mathcal{L}_k$  of order k-triples to be tested for  $k=0,\ldots,N-2$ . Conditional independence test T at significance level  $\alpha$ .

```
\begin{array}{l} \textbf{if } \mathcal{G}_0 \\ \textbf{is Markov equivalence class then} \\ \mathcal{G}_0 \leftarrow \textbf{member of } \mathcal{G}_0; \\ \textbf{end if} \\ v = 0.0; \\ \textbf{for } k = 0, \dots, N-2 \ \textbf{do} \\ v_k = 0.0; \\ \textbf{count} = 0; \\ \textbf{for triples } (X,Y,\mathcal{S}) \in \mathcal{L}_k \ \textbf{do} \\ \textbf{count} += 1; \\ v_k += |\text{Oracle}_{\mathcal{G}_0}(X,Y,\mathcal{S}) - \text{testresult}_{(T,\alpha)}(X,Y,\mathcal{S})|; \\ \textbf{end for} \\ v += \frac{v_k}{\text{count}}; \\ \textbf{end for} \\ \textbf{return } \frac{v}{N-1}. \end{array}
```

#### **Algorithm 6** Pseudocode to compute Markov obscurity (c-obscurity).

**Require:** Causal graph  $\mathcal{G}_0$  (e.g. DAG) or Markov equivalence class (e.g. CPDAG) with N nodes, Oracle for fitting notion of separation. Sets  $\mathcal{L}_k$  of order k-triples to be tested for  $k=0,\ldots,N-2$ . Conditional independence test T at significance level  $\alpha$ .

```
if \mathcal{G}_0 is Markov equivalence class then
    \mathcal{G}_0 \leftarrow \text{member of } \mathcal{G}_0;
end if
v = 0.0;
for k = 0, ..., N - 2 do
    v_k = 0.0;
    count = 0;
    for triples (X, Y, \mathcal{S}) \in \mathcal{L}_k do
       if \operatorname{Oracle}_{\mathcal{G}_0}(X,Y,\mathcal{S}) == 0 then
            count += 1;
           if \operatorname{testresult}_{(T,\alpha)}(X,Y,\mathcal{S}) == 1 then
                v_k += 1;
            end if
       end if
    end for
v \mathrel{+}= \frac{v_k}{\mathrm{count}}; end for
return \frac{v}{N-1}.
```

# Algorithm 7 Pseudocode to compute Faithfulness obscurity (s-obscurity).

```
Require: Causal graph \mathcal{G}_0 (e.g. DAG) or Markov equivalence class (e.g. CPDAG) with N nodes, Oracle for fitting
   notion of separation. Sets \mathcal{L}_k of order k-triples to be tested for k=0,\ldots,N-2. Conditional independence test T
   at significance level \alpha.
   if \mathcal{G}_0 is Markov equivalence class then
      \mathcal{G}_0 \leftarrow \text{member of } \mathcal{G}_0;
   end if
   v = 0.0;
   for k=0,\ldots,N-2 do
      v_k = 0.0;
      count = 0;
      for triples (X, Y, S) \in \mathcal{L}_k do
         if \operatorname{Oracle}_{\mathcal{G}_0}(X,Y,\mathcal{S}) == 1 then
             count += 1;
            if \operatorname{testresult}_{(T,\alpha)}(X,Y,\mathcal{S}) == 0 then
                v_k += 1;
             end if
         end if
      end for
      v \mathrel{+}= \frac{v_k}{\mathrm{count}};
   end for
   return \frac{v}{N-1}.
```

# **Appendix F** Additional Figures

This section contains additional figures referring to Subsections 3.1 and 3.5.

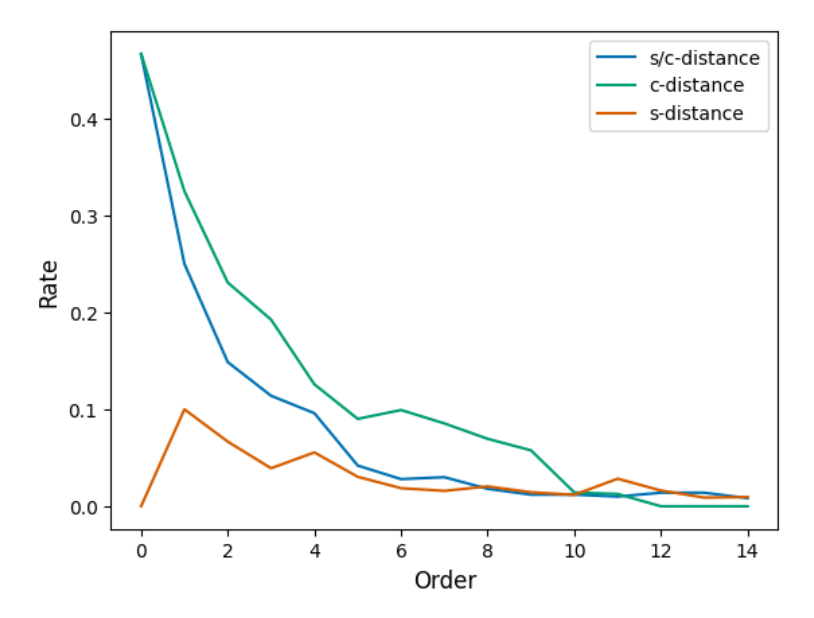


Figure 13: Values of  $d_{s/c}(\mathcal{G},\mathcal{H}), d_c(\mathcal{G},\mathcal{H})$  and  $d_s(\mathcal{G},\mathcal{H})$  in the example of Figure 2 at M=8 (16 nodes) for different values of k. To compute  $d_{s/c}$  and  $d_c$ , we drew 500 triples randomly for higher order terms (k>2).

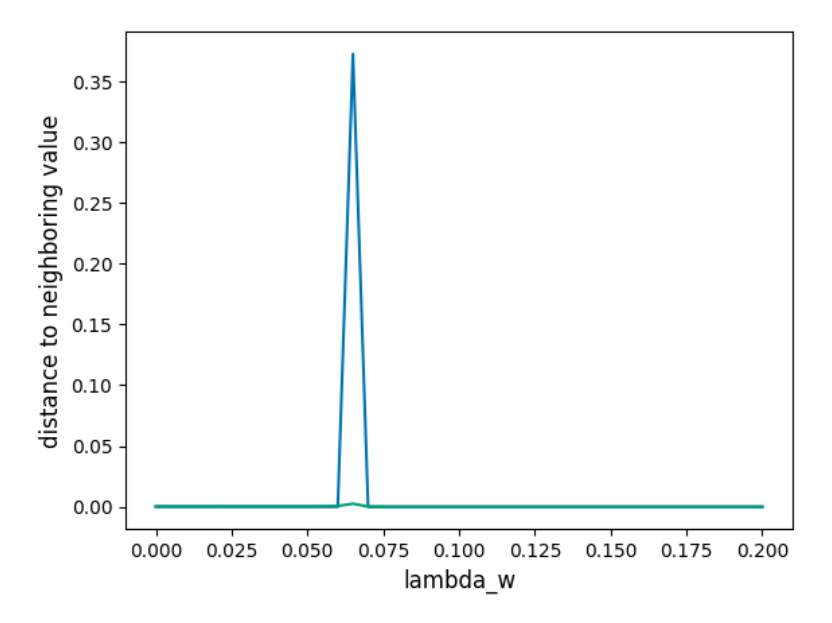


Figure 14: For each value of the regularization parameter  $\lambda_w$  of the DYNOTEARS algorithm, we plot  $d_{s/c}(\mathcal{G}_{\lambda_w},\mathcal{G}_{\lambda_w+0.005})$  and  $\widetilde{SHD}(\mathcal{G}_{\lambda_w},\mathcal{G}_{\lambda_w+0.005})$  to see how strongly the inferred graph changes when  $\lambda_w$  is increased. The remaining hyperparameters are set to  $\tau_m ax = 5$ ,  $w_{thresh} = 0.1$  and  $\lambda_a = 0.05$ . There is only one phase transition to another graph at between  $\lambda_w = 0.065$  and  $\lambda_w = 0.07$ . This transition is barely noticeable in SHD but fundamental in s/c-distance as more than 35% of separation/connection statements change.